Senolytic activity of small molecular polyphenols from olive restores chondrocyte redifferentiation and promotes a pro-regenerative environment in osteoarthritis

Marta Varela-Eirín[1], Paula Carpintero-Fernández[1], Agustín Sánchez-Temprano[1], Adrián Varela-Vázquez[1], Carlos Luis Paíno[2], Antonio Casado-Díaz[3], Alfonso Calañas Continente[3], Virginia Mato[4], Eduardo Fonseca[1], Mustapha Kandouz[5], Alfonso Blanco[6], José Ramón Caeiro[7], María D. Mayán[1]

[1]CellCOM Research Group, Instituto de Investigación Biomédica de A Coruña (INIBIC), Servizo Galego de Saúde (SERGAS), Universidade da Coruña (UDC), A Coruña, Spain
[2]Neurobiology-Research Service, Hospital Universitario Ramón y Cajal (IRYCIS), Madrid, Spain
[3]UGC Endocrinology and Nutrition, Maimónides Biomedical Research Institute of Córdoba (IMIBIC), Hospital Universitario Reina Sofía – CIBERFES, Universidad de Córdoba, Córdoba, Spain
[4]Centre for Medical Informatics and Radiological Diagnosis, Universidade da Coruña, A Coruña, Spain
[5]Department of Pathology, School of Medicine, Wayne State University, Detroit, MI 48202, USA
[6]Flow Cytometry Core Technologies, UCD Conway Institute, University College Dublin, Dublin, Ireland
[7]Department of Orthopaedic Surgery and Traumatology, Complexo Hospitalario Universitario de Santiago de Compostela (CHUS), Universidade de Santiago de Compostela (USC), Choupana s/n, Santiago de Compostela, Spain

Correspondence to: María D. Mayán; **email:** Ma.Dolores.Mayan.Santos@sergas.es
Keywords: senescence, dedifferentiation, osteoarthritis, connexin43, tissue regeneration
Received: March 18, 2020   **Accepted:** July 13, 2020   **Published:** August 3, 2020

ABSTRACT

Articular cartilage and synovial tissue from patients with osteoarthritis (OA) show an overactivity of connexin43 (Cx43) and accumulation of senescent cells associated with disrupted tissue regeneration and disease progression. The aim of this study was to determine the effect of oleuropein on Cx43 and cellular senescence for tissue engineering and regenerative medicine strategies for OA treatment. Oleuropein regulates Cx43 promoter activity and enhances the propensity of hMSCs to differentiate into chondrocytes and bone cells, reducing adipogenesis. This small molecule reduce Cx43 levels and decrease Twist-1 activity in osteoarthritic chondrocytes (OACs), leading to redifferentiation, restoring the synthesis of cartilage ECM components (Col2A1 and proteoglycans), and reducing the inflammatory and catabolic factors mediated by NF-kB (IL-1ß, IL-6, COX-2 and MMP-3), in addition to lowering cellular senescence in OACs, synovial and bone cells. Our *in vitro* results demonstrate the use of olive-derived polyphenols, such as oleuropein, as potentially effective therapeutic agents to improve chondrogenesis of hMSCs, to induce chondrocyte re-differentiation in OACs and clearing out senescent cells in joint tissues in order to prevent or stop the progression of the disease.

INTRODUCTION

Articular cartilage from patients with osteoarthritis (OA) shows accumulation of dedifferentiated and senescent cells [1–4] together with increased inflammation and breakdown of cartilage extracellular matrix (ECM) [5]. Importantly, cartilage and synovial tissue from OA patients contain high levels of the gap

junction protein connexin43 (Cx43). Targeting Cx43 might be a promising approach to treat several age-related and chronic degenerative diseases by modulating tissue regeneration, inflammation and response to injury [6]. Cx43 belongs to the integral membrane protein family called connexins, that enable direct communication between neighboring cells via hemichannels, gap junctions, extracellular vesicles and tunneling nanotubes [7]. Additionally, connexins act as signaling hubs regulating different signaling pathways via their cytoplasmic domains [2, 8]. Cx43 is the major Cx protein expressed in chondrocytes, synovial cells (SC) and bone cells (BC) [9–11] and it has been involved in normal development and function of joint tissues [12, 13] and joint disorders [9–11, 14, 15]

During tissue regeneration and following injury, dedifferentiation, redifferentiation and senescence processes play finely tuned temporal and spatial roles to reverse the loss [2, 16]. In addition, accumulation of senescent cells is described to play a major role in OA progression [1, 17–22]. Cellular senescence is a stable cell-cycle arrest with increased expression of cell cycle inhibitors such as p16^{INK4A} and enhanced synthesis of the senescence-associated secretory phenotype (SASP) factors, which mainly consist of inflammatory cytokines and ECM degrading enzymes, among other factors [23]. The elimination of senescent cells using senolytics has been described to attenuate cartilage and joint degeneration in OA [1, 24–26]. In fact, some of these drugs including UBX0101 and the natural-occurring flavone Fisetin [27, 28] with potential senolytic activity are currently under clinical trial for OA treatment (NCT04210986; NCT04349956; NCT04229225; NCT04129944) [29–32].

Cx43 has been involved in different phases of tissue regeneration including chronic inflammation, cell differentiation and cellular senescence [33, 34]. Overexpression of Cx43 and enhanced gap junction intercellular communication (GJIC) in osteoarthritic chondrocytes (OACs) compromise their ability to re-differentiate, promoting a stem-like state by activating Twist-1, which leads to dedifferentiation via epithelial-to-mesenchymal transition (EMT) [2]. However, we have also previously observed that high levels of Cx43 lead to p53/p21-mediated cellular senescence [2]. Increased levels of Cx43 in OA cartilage is extensively described in the literature [9, 11, 35–37], as well as the presence of dedifferentiation (stem-like state) and proliferative chondrocytes [4, 38–44] together with the accumulation of senescent cells [1, 18, 20, 29], indicating that both phenotypes, dedifferentiated and senescent chondrocytes, co-exist in cartilage from OA patients and contribute to the progression of the disease. However, we have recently demonstrated that

downregulation of Cx43 reduces stemness and accumulation of senescent cells, indicating that Cx43 acts as a molecular switch in the phenotype of chondrocyte within a wound healing process [2]. In fact, downregulation of Cx43 in different wound healing and age-related disorders halts disease progression by restoring tissue regeneration [45–47].

Oleuropein is the most abundant polyphenol in the leaves and fruit of the olive plant and is a potent antioxidant agent with anti-tumour and anti-inflammatory properties [48, 49]. The mechanism of action of this polyphenol is under investigation [48]. Some studies showed that oleuropein and its major metabolite hydroxytyrosol have antioxidant activity by inhibition and/or scavenging of ROS [50], which can reduce NF-kB activation [51, 52]. Other mechanistic studies implicate nitric oxide (NO) production [53, 54] or autophagy and inhibition of the mammalian target of rapamycin (mTOR) [55, 56]. A gene expression profiling study has suggested that oleuropein affects the expression of genes involved in oxidative stress, inflammation, fibrosis, cell proliferation or differentiation [57], suggesting that the beneficial effects of this molecule may be multifactorial and context-dependent [57]. Innovative approaches based on functional foods have been recently studied and many beneficial effects of dietary olive oil on human health were already described [58–62]. In fact, extra virgin olive oil and olive leaf extract supplemented diets have been shown to reduce inflammation and preserve cartilage, muscle and joint function in rat preclinical models of OA [63–68].

In this study, we have used a small-scale screening to identify compounds that downregulate Cx43. Here we describe the use of small molecules based on olive phenolic compounds to downregulate Cx43 in OA by using 2D and 3D human cartilage models. We have found that oleuropein decreases Cx43 promoter activity and GJIC, thus enhancing osteogenesis and chondrogenesis in hMSCs and redifferentiation of OACs. Beside downregulation of Cx43, olive-derived small polyphenols reduce cellular senescence in OACs, BC and SC, in addition to inflammatory and catabolic activities related to cartilage degradation in OA patients.

RESULTS

Olive-derived polyphenols impair adipogenesis and enhance the chondrogenic and osteogenic ability of hMSCs

We used a small-scale screening to identify compounds that downregulate Cx43 (data not shown), and we identified the small molecule oleuropein

(Figure 1A). Oleuropein and an olive-extract (OE) significantly reduced Cx43 protein levels in OACs (Figure 1A). MTT assays showed no effect of 0.1-10 µM oleuropein on cell viability of primary chondrocytes and hMSCs (Supplementary Figure 1). Based on these results and other studies [69], 10 µM was selected as the highest concentration with no toxic effect after 17 h in culture.

We next examined hMSCs differentiation capacity in the presence of oleuropein (Figure 1B, 1C and Supplementary Figure 2). In accordance with previous results [69], oleuropein-treated hMSCs showed significantly less adipogenic differentiation ability, whereas osteogenesis was significantly increased (Figure 1B and Supplementary Figure 2A, 2B). Furthermore, a 3D micromass culture system using chondrogenic medium supplemented with 10 µM oleuropein or OE revealed increased ECM properties, reflecting a greater degree of chondrogenic differentiation, with higher levels of Col2A1 deposition and increased levels of aggrecan (ACAN) gene expression (Figure 1C and Supplementary Figure 2C). Remarkably, decreased Cx43 gene expression was detected in hMSCs during differentiation, mainly during chondrogenesis (Figure 1D, 1E and Supplementary Figure 3A). We have also observed changes in Cx43 phosphorylation pattern at 7 and 14 days of chondrogenic differentiation (Figure 1D), which can affect Cx43 stability and channel activity. Different Cx43 phosphorylation patterns were also detected during adipogenesis and osteogenesis, suggesting differential regulation of Cx43 during hMSCs differentiation (Supplementary Figure 3B). The treatment of hMSCs during chondrogenic differentiation with oleuropein for 14 days caused an additional 1.7 fold reduction in Cx43 gene expression (Figure 1E).

In concordance with these results, OACs' redifferentiation for 7 days with oleuropein decreased Cx43 protein levels, but it did not affect its phosphorylation pattern (Figure 1F). However, we did not observe changes in the phosphorylation pattern when hMSCs or chondrocytes were treated with oleuropein (Figure 1F and Supplementary Figure 4A).

It is important to note that these results were obtained during differentiation of hMSCs under osteogenesis or chondrogenesis (Figure 1B–1E) and dedifferentiated OACs in normal and in chondrogenic medium (Figure 1A and 1F). However, the treatment of undifferentiated hMSCs cultured in basal growth medium with oleuropein/OE increased Cx43 levels (Supplementary Figure 4A and 4B) and GJIC (Supplementary Figure 4C), indicating that the effect of these olive derived polyphenols may be different depending on the cellular context.

Downregulation of Cx43 activity by oleuropein downregulates Twist-1 and enhances redifferentiation of OACs

Oleuropein modulation of Cx43 significantly reduced GJIC in OACs (Figure 2A), but not in healthy chondrocytes (Figure 2B). The decrease in Cx43 and GJIC was correlated with a significant reduction in the levels of the stemness markers CD105 and CD166 (Figure 2C). This result was consistent with our previous observations, where CD105 and CD166 were reduced when Cx43 was downregulated or when OACs were redifferentiated. In fact, oleuropein effectively improved the OACs phenotype, detected by the increase of Col2A1 levels and the decrease of proinflammatory mediators and MMP-3 levels (Figure 2D, 2E). Oleuropein treatment reduced overall Cx43 positivity, increased Col2A1 levels (Figure 2D) and decreased interleukin 6 (IL-6), COX-2, IL-1ß and MMP-3 gene expression (Figure 2E) and protein levels (Figure 2F).

Next, we sought to confirm whether oleuropein would target chondrocyte plasticity in 3D cultures. Treatment of OACs grown as a 3D culture in chondrogenic medium with oleuropein increased the deposition of proteoglycans and Col2A1 (Figure 3A), improving the ECM structure by decreasing Cx43 levels (Figure 3B).

To explore the effect of oleuropein on cell plasticity, OACs were grown in adipogenic medium supplemented with oleuropein, which significantly decreased their adipogenic differentiation (Figure 3C). However, oleuropein promoted osteogenesis when OACs were grown in osteogenic medium supplemented with 10 µM of oleuropein (Supplementary Figure 5).

Upregulation of Cx43 in OA involves dedifferentiation via chondrocyte-to-mesenchymal transition by Twist-1 activation, which was also reported in OA cartilage [2, 70, 71]. OACs were treated with the arthritic insult oligomycin, which induces cellular ROS production and cartilage degradation [72, 73]. After oleuropein treatment, OACs showed a significant reduction in the nuclear localization of Twist-1 (Figure 3D). Nuclear localization of Twist-1 in the presence of oligomycin was attenuated when Cx43 protein levels were reduced by oleuropein treatment of OACs (Figure 3E). In addition, oleuropein treatment in OACs reduced the expression of the mesenchymal and EMT markers N-cadherin and vimentin (Figure 3F).

Oleuropein modulates Cx43 gene promoter activity

In chondrocytes, decreased Cx43 protein levels were detected when OACs and the T/C-28a2 cell line were treated with oleuropein (Figures 1A and 4A). However,
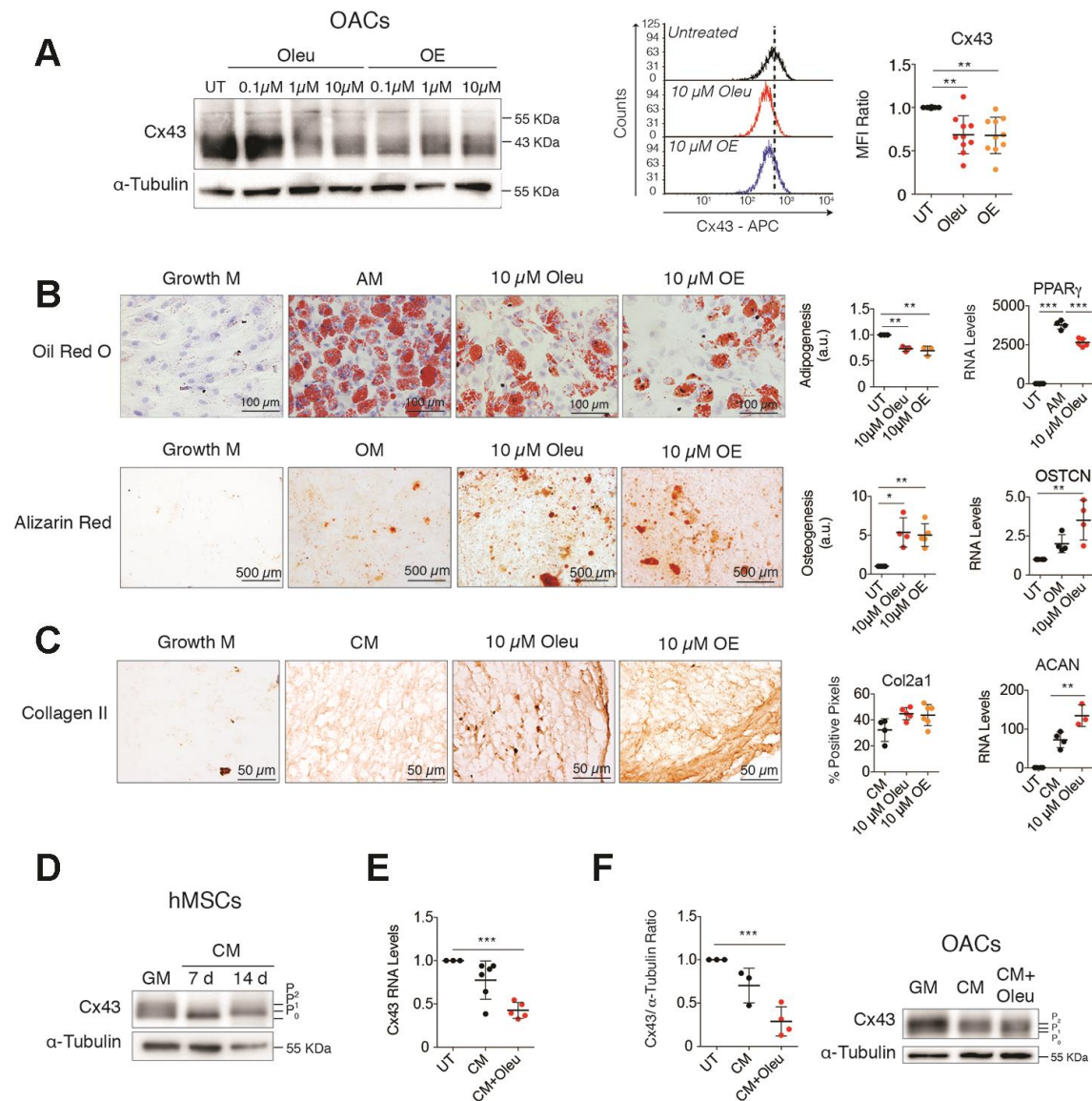
Figure 1. Downregulation of Cx43 during chondrogenesis improves differentiation towards chondrocytes. (**A**) Treatment of OACs with oleuropein (Oleu) or olive extract (OE) for 2 h significantly downregulates Cx43 protein detected by western-blot and flow cytometry. Median fluorescence intensity (MFI) ratios of oleuropein and OE treatments with respect to their untreated controls of each experiment are represented (n=10 independent experiments, *P*=0.0003). (**B**) Differentiation capacity of hMSCs isolated from bone marrow grown in adipogenic (top, 21 days) or osteogenic (bottom, 21 days) medium supplemented with 10 μM oleuropein or 10 μM OE. hMSCs cultured in growth medium were used as a control. Top, adipogenic evaluation by oil red O for lipid staining and by PPARγ gene expression. Data represent the ratio of cells containing lipid deposits to the total number of cells (n=3 independent experiments, *P*<0.0001). Values were normalized to hMSCs differentiated in adipogenic medium without treatment (AM). On the right, PPARγ gene expression (n=4 independent experiments, *P*<0.0001). Alizarin red staining was used to detect calcium deposits for osteogenic differentiation. Values were obtained by counting red pixels and normalized to those of hMSCs differentiated in osteogenic medium without treatment (OM) (n=4-6 independent experiments, *P*=0.0317). OSTCN gene expression was measured to confirm osteogenic differentiation (n=4 independent experiments, *P*=0.0055). (**C**) Differentiation capacity of hMSCs isolated from bone marrow grown in chondrogenic medium as micromasses for 30 days. Representative images for Col2A1. The quantification is shown on the right (n=5–6 micromasses from independent experiments, *P*=0.0423). Chondrogenesis was also evaluated by ACAN gene expression quantification (n=3–4 independent experiments, *P*<0.0001). (**D**) Cx43 protein levels in hMSCs, isolated from bone marrow and from inguinal fat, differentiated for 7 and 14 days in the presence of chondrogenic medium (CM) in comparison to untreated hMSCs cultured in normal growth medium (GM). (**E**) Cx43 RNA expression of hMSCs cultured for 14 days in the presence of chondrogenic medium (CM) alone or supplemented with 10 μM oleuropein. Data were normalized to HPRT-1 levels (n=5-6 independent experiments, *P*<0.0001). (**F**) Cx43 protein levels were analyzed by western blot in OACs differentiated for 7 days in the presence of chondrogenic medium (CM), supplemented with 10 μM oleuropein. The graph represents the quantification from 3 independent experiments (*P*=0.0004). Data is expressed as mean±SD, one-way ANOVA; *P<0.05, **P<0.01 and ***P<0.0001.
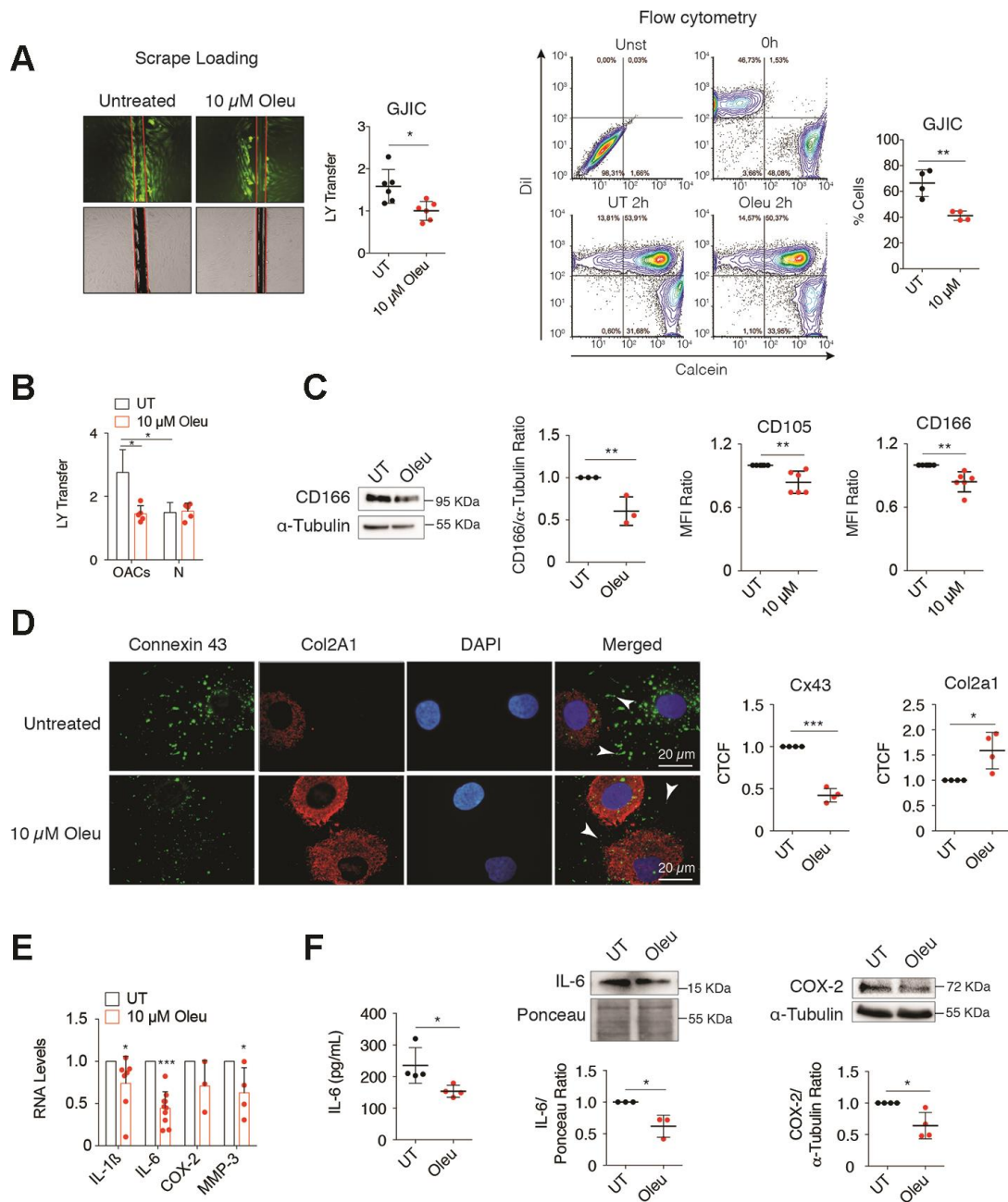
Figure 2. Downregulation of Cx43 by oleuropein decreases GJIC and improves the phenotype of OACs. (**A**) Oleuropein (Oleu) treatment significantly decreases GJIC evaluated by an SL/DT assay when OACs were exposed with this molecule for 2 h (top, n=6 independent experiments; Student's *t* test, *P*<0.0001). The results were confirmed by calcein transfer by flow cytometry (n=4 independent experiments; Student's *t* test, *P*=0.0037). (**B**) Graph showing the effect of oleuropein on GJIC when healthy chondrocytes (N) were exposed to 10 μM oleuropein compared with OACs (n=5 independent experiments; one-way ANOVA, *P*=0.0004). (**C**) OACs cultured for 7 days with 10 μM Oleu showed reduced expression of the mesenchymal markers CD105 and CD166, analyzed by flow cytometry. Student's *t* test, *P*=0.0039 (CD105) and *P*=0.0022 (CD166), n=6 independent experiments. CD166 levels were also analyzed by western blot (n=3 independent experiments, Student's *t* test, *P*=0.0046). (**D**) Downregulation of Cx43 increased Col2A1, detected by immunofluorescence in OACs treated with 10 μM oleuropein. Graphs represent the corrected total cell fluorescence (CTCF) of Cx43 and Col2a1 (n=4 independent experiments). Student's *t* test, *P*<0.0001 (Cx43), and *P*=0.0007 (Col2a1). (**E**) mRNA levels of IL-1ß, IL-6, COX-2 and MMP-3 of OACs cultured in normal medium (UT) exposed to 10 μM oleuropein for 2 h. n=4–7 independent experiments. Student's *t* test: *P*= 0.033 (IL-1ß), *P*<0.0001 (IL-6), *P*=0.1013 (COX-2), *P*=0.0466 (MMP-3). (**F**) IL-6 detected by ELISA when OACs were treated with oleuropein for 72 h (n=4 independent experiments, Student's *t* test, *P*=0.0345). IL-6 (n=3 independent experiments) and COX-2 (n=4 independent experiments) protein levels detected by western-blot in OACs treated with 10 μM oleuropein for 72 h. Student's *t* test, *P*=0.0193 (IL-6), *P*=0.0141 (COX-2). Data is expressed as mean±SD; *P*<0.05, **P*<0.01 and ***P*<0.0001.

these changes were not evident in treated Cx43-overexpressing T/C-28a2 chondrocytes (Figure 4A, bottom), suggesting that oleuropein may affect Cx43 gene promoter activity rather than protein stability. We thus measured whether oleuropein affected the activity of the Cx43 gene promoter using a real-time reporter system. T/C-28a2 chondrocytes were transfected with a firefly luciferase reporter vector containing the regulatory regions of the Cx43 promoter and incubated for 1 h with oleuropein and the mitochondrial inhibitor oligomycin, which enhanced Cx43 gene expression (Figures 3E, 4B). Cx43 promoter activity decreased after oleuropein treatment (Figure 4B), while oligomycin increased the luminescence signal, and the effect of oligomycin was significantly attenuated in the presence of oleuropein (Figure 4B), which was correlated with Cx43 gene expression (Figure 4B). Luminescence signal strongly correlated with the effects
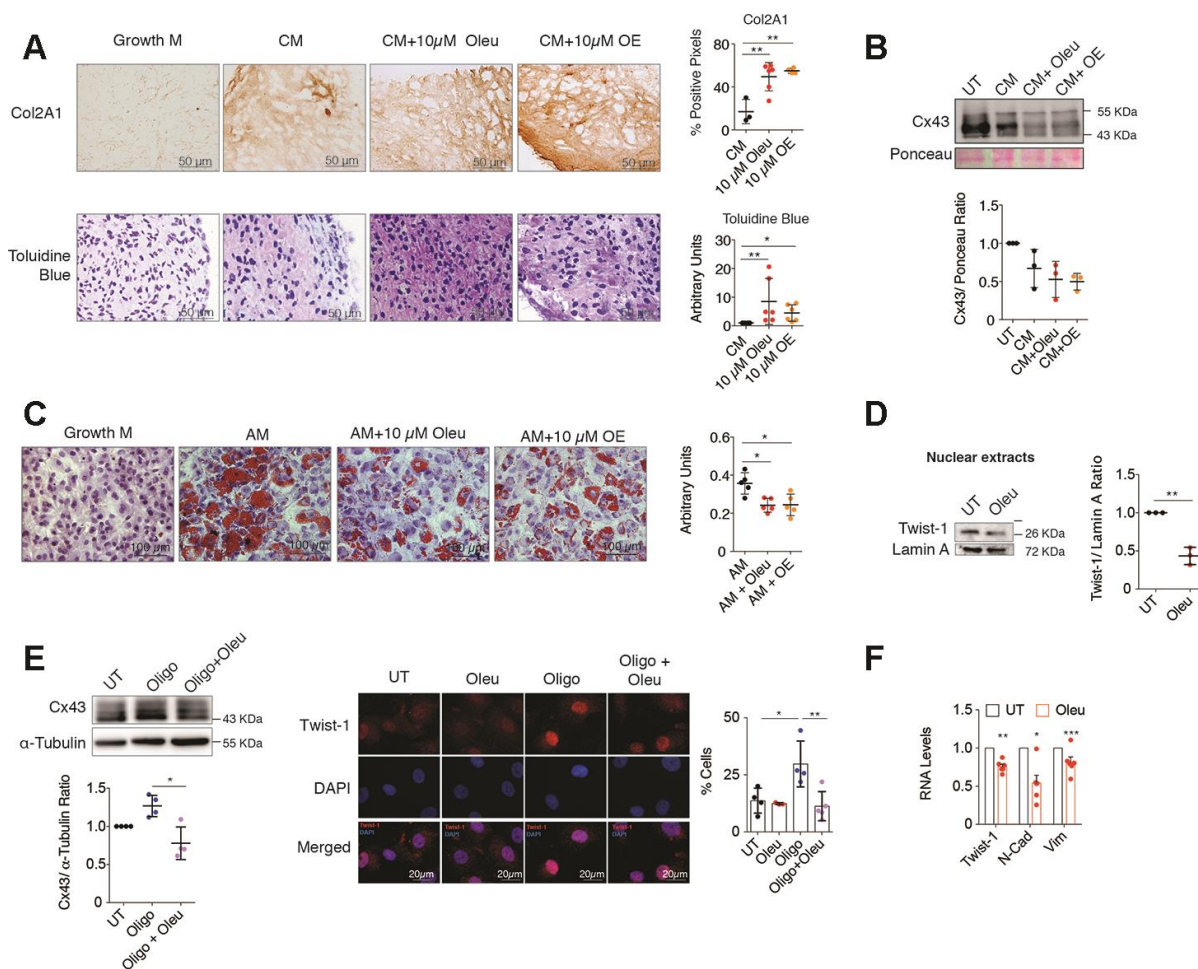

Figure 3. Oleuropein treatment enhances chondrocyte redifferentiation. (**A**) Immunohistochemistry of Col2A1 (4-6 independent experiments; one-way ANOVA, *P*=0.0019) and toluidine blue staining of proteoglycan subunits (n=6 independent experiments; one-way ANOVA, *P*=0.059) indicate significant enrichment in ECM components in OACs micromasses grown in 3D culture for 30 days in chondrogenic medium (CM) when supplemented with 10 μM oleuropein (Oleu) or OE. (**B**) Cx43 protein levels detected by western blot (and normalized to Ponceau staining) are reduced when OACs micromasses are exposed to CM supplemented with 10 μM oleuropein or OE for 21 days (n=3 independent experiments; one-way ANOVA, *P*=0.0328). (**C**) Oil red staining showing reduced OACs dedifferentiation upon exposure to Oleu or OE in adipogenic medium (n=5 independent experiments; one-way ANOVA, *P*=0.0001). (**D**) Nuclear levels of Twist-1 were decreased in OACs cultured with 10 μM oleuropein for 2 h. Lamin A was used as a loading control (n=3 independent experiments; Student's *t* test, *P*=0.001). (**E**) Cx43 protein levels in primary OACs after 1-h treatment with oleuropein or oligomycin. Western blot represents n=4 independent experiments. Quantification is shown on the right (one-way ANOVA, *P*=0.0036). On the right, immunofluorescence for Twist-1 (red) in primary OACs treated with 5 μg/ml oligomycin and 10 μM oleuropein for 1 h. The graph represents the percentage of cells with Twist-1 nuclear localization (n=4 independent experiments; one-way ANOVA, *P*=0.0067). (**F**) The mRNA expression of the EMT markers Twist-1, N-Cadherin and Vimentin in OACs treated with 10 μM oleuropein for 2 h. Data were normalized to HPRT-1 levels. n= 5 independent experiments; Student's *t* test*: P*<0.0001 (Twist-1), *P*= 0.0011 (N-Cad), *P*=0.0209 (Vim). Data is expressed as mean±SD; **P*<0.05, ***P*<0.01 and ****P*<0.0001.

of oleuropein and oligomycin on protein levels (Figures 3E and 4C). These results indicate that oleuropein affects Cx43 gene promoter activity, thus downregulating Cx43 protein levels (Figure 1A and Figure 4A–4C) and GJIC in OACs (Figure 2B).

Oleuropein enhances elimination of senescent cells

Senescent cells through their secretory activity (SASP) can promote dedifferentiation and reprogramming in neighboring cells in the context of tissue injury [74]. OACs treated with 10 µM oleuropein for 7/14 days in growth medium showed a significant reduction of senescent cells accumulated after 5 days of primary culture (Figure 5A). Consistent with these models,

Cx43 upregulation due to the oligomycin insult significantly contributed to increase cellular senescence in OACs accumulated after 5 days in monolayer (Figure 5B, left), whereas co-treatment with oleuropein significantly halted the accumulation of senescent cells after 24 h (Figure 5B, left) and 7 days under treatment (Figure 5B, right). Interestingly, increased SA-βGal activity was detected when the T/C-28a2 chondrocytes were treated with bleomycin to induce cellular senescence for 24 h, while the exposure to oleuropein for 24 h reduced the number of senescent cells (Supplementary Figure 6B). In accordance with these results, treatment of OACs with oleuropein led to decreased levels of the senescence biomarkers p16[INK4A] (Figure 5C) and p53/p21 (Figure 5D). Furthermore, the
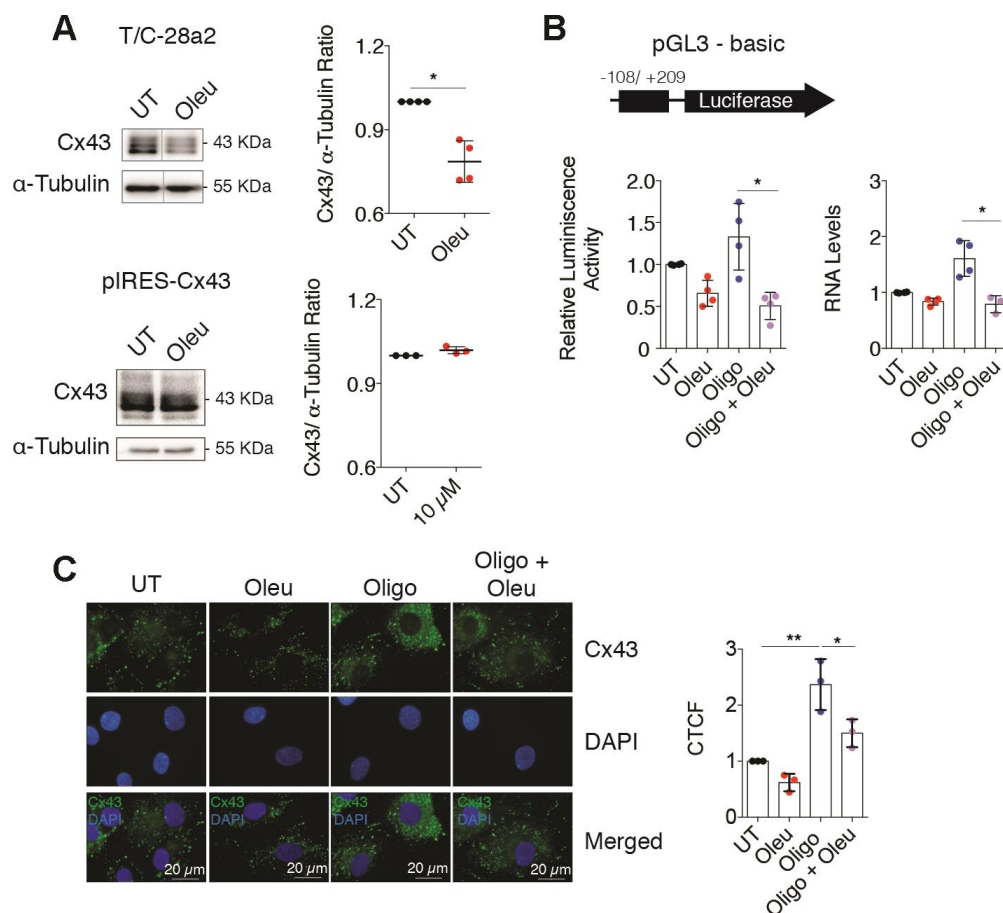

Figure 4. Oleuropein modulates the Cx43 promoter activity in chondrocytes. (**A**) Treatment with 10 µM oleuropein for 2 h decreases Cx43 protein levels in T/C-28a2 cells (n=4 independent experiments, Student's *t* test, *P*=0.0012), but this effect was not observed in the same cell line overexpressing Cx43 (pIRES-Cx43)(n=3 independent experiments, Student's *t* test, *P*=0.0624). (**B**) Luciferase reporter assay indicating that oleuropein inhibits Cx43 promoter activity. The graphs indicate the normalized luminescence activity in the T/C-28a2 transfected with a pGL3-basic plasmid containing 300 base pairs of Cx43 promoter ligated to the luciferase gene. Cells were cultured in DMEM with 10% FBS (UT) and with 5 µg/ml oligomycin or 10 µM oleuropein for 1 h as indicated (n=4 independent experiments; one-way ANOVA, *P*=0.0012). On the right, Cx43 gene expression under 5 µg/ml oligomycin and 10 µM oleuropein treatment in OACs treated for 1 h (n=4 independent experiments; one-way ANOVA, *P*=0.0002). Data were normalized to HPRT-1 levels. (**C**) Immunofluorescence assays of Cx43 in OACs treated with 10 µM oleuropein or 5 µg/ml oligomycin for 1 h. Data were normalized to the untreated condition (n=3 independent experiments; one-way ANOVA, *P*<0.0001). Data is expressed as mean±SD; *P<0.05, **P<0.01 and ***P<0.0001.

proliferative arrest observed after the treatment of T/C-28a2 healthy chondrocytes with the Cyclin-Dependent Kinase 4/6 inhibitor palbociclib to induce senescence was partially inhibited by the co-treatment with oleuropein (Figure 5E). Oleuropein reduced the accumulation of senescent cells and attenuated the oligomycin-induced SASP secretion detected by IL-6, COX-2 and IL-1ß gene expression in chondrocytes (Figure 5F). The SASP, including IL-6 gene expression, can be activated by NF-κB [75]. Oleuropein protected from the increase of Cx43 under TNFα treatment (Figure 5G, left), and NF-κB (p65) activation by TNFα in OACs was diminished when cells were exposed to oleuropein for 1 h (Figure 5G). Further, NF-κB nuclear translocation was partially abolished in OACs treated with oleuropein for only 2 h (Figure 5H).

To further test the senolytic activity of oleuropein, SC and BC from OA patients were treated with oleuropein (Figure 6). We observed decreased Cx43 protein levels after oleuropein exposure (Figure 6A and 6D), together with a significant reduction in senescent cells accumulated after 5 days in primary culture (Figure 6B and 6E), confirmed by p16^{INK4A} gene expression and the synthesis of the SASP factors IL-1ß, COX-2 and IL-6 (Figure 6C and 6F).

DISCUSSION

Previous data from our group demonstrate that Cx43 downregulation improves the chondrocyte phenotype, protecting chondrocytes from dedifferentiation and senescence [2]. Although oleuropein and olive-based diets were reported to protect from OA progression [76, 77], there was no solid evidence about its underlying molecular mechanisms. In our study, we show that oleuropein modulates Cx43 gene promoter activity, reducing Cx43 and GJIC in OACs. Indeed, our data indicate that Cx43 downregulation by oleuropein in OACs improves cell phenotype by protecting chondrocytes from Twist-1 activation and from accumulation of senescent cells (Figures 2, 3, 5 and 6). This is the first study that demonstrated one of the potential mechanisms of oleuropein in OACs, SC and BC (Figures 5 and 6) from patients, and in hMSCs (Figure 1), with relevant applications in regenerative medicine.

Our results show that the effects of oleuropein are often equal or even smaller than those of the olive extract, suggesting that other compounds may synergize with oleuropein activity in chondrocytes [78]. On the other hand, the treatment of hMSCs with oleuropein or OE during differentiation leads to downregulation of Cx43 and GJIC, enhancing osteogenesis and chondrogenesis, but reducing adipogenesis. This differential sensitivity

of hMSCs to oleuropein and OE may have potential applications in preventive and regenerative medicine in other bone and cartilage disorders.

Our data show decreased Cx43 and GJIC levels in the presence of oleuropein in OACs and in differentiating hMSCs, but increased Cx43 and GJIC levels in undifferentiated hMSCs, suggesting that the effect of this molecule on GJIC depends on its effect on Cx43 levels (or subcellular localization). In fact, phosphorylation of Cx43 affects protein stability and GJIC activity [79] and we have detected changes in Cx43 phosphorylation pattern during hMSCs differentiation but not under oleuropein treatment indicating that oleuropein affects Cx43 levels more than gap junction plaque activity or modulation. We cannot therefore discard that the effect of oleuropein may also depend on channel-independent activities, which involve the signaling hub's ability of Cx43 to recruit proteins to the membrane [34, 80, 81] or its ability to control gene transcription [82]. It is important to note that oleuropein may have other targets that may contribute to the drug effect. Despite this limitation and based on our results, we expect that the effect of oleuropein occurs at least partially through Cx43 modulation. Here, we show that oleuropein restores chondrocyte phenotype detected by reduced levels of the stem-markers CD105, CD166, N-cad and vimentin (Figure 2C, 3F). The effect of oleuropein in chondrocyte plasticity correlated with activation of redifferentiation via downregulation of Cx43 and Twist-1 (Figure 3D–3F), leading to increased levels of proteoglycans and Col2A1 together with decreased levels of inflammatory cytokines and metalloproteinases (Figures 2D–2G, and 3A).

In cell culture and in cartilage, OACs undergo dedifferentiation and senescence [2, 18, 20]. Elimination of senescent cells *in vivo* using the senolytic drug UBX0101 has been demonstrated to improve cartilage regeneration after articular joint injury in mice [1]. Here we show that oleuropein reduces cellular senescence in OACs, SC and BC and protects from accumulation of senescent cells under an arthritic insult (Figures 5A, 5B, 6B and 6F). NF-kB has been shown to regulate the inflammatory components of the SASP, together with other factors [83, 84]. In this study the reduction of senescence is accompanied by reduced NF-kB activity, and therefore reduced synthesis of SASP (Figure 5F). Notably, these components enhance inflammation, senescence and activate dedifferentiation and cellular reprogramming of nearby non-senescent cells (e.g. via IL-6) [74], contributing to the stem-like state of chondrocytes in OA and to the accumulation of senescent cells. Accordingly, we have previously reported that upregulation of Cx43 leads to p53/p16 upregulation and senescence [2]. Using the T/C-28a2 cells with a Cx43 overexpression vector and a

CRISPR/Cas9-mediated heterozygous Cx43 gene knockdown cell line we have demonstrated that Cx43 is an upstream effector of both senescence (involving p53 and p16 pathways) and NF-kB activation [2].

Cellular reprogramming, dedifferentiation via EMT and senescence play active roles during tissue regeneration [85, 86]. Accumulation of dedifferentiated (stem-like cells) and senescent cells leads to impaired tissue
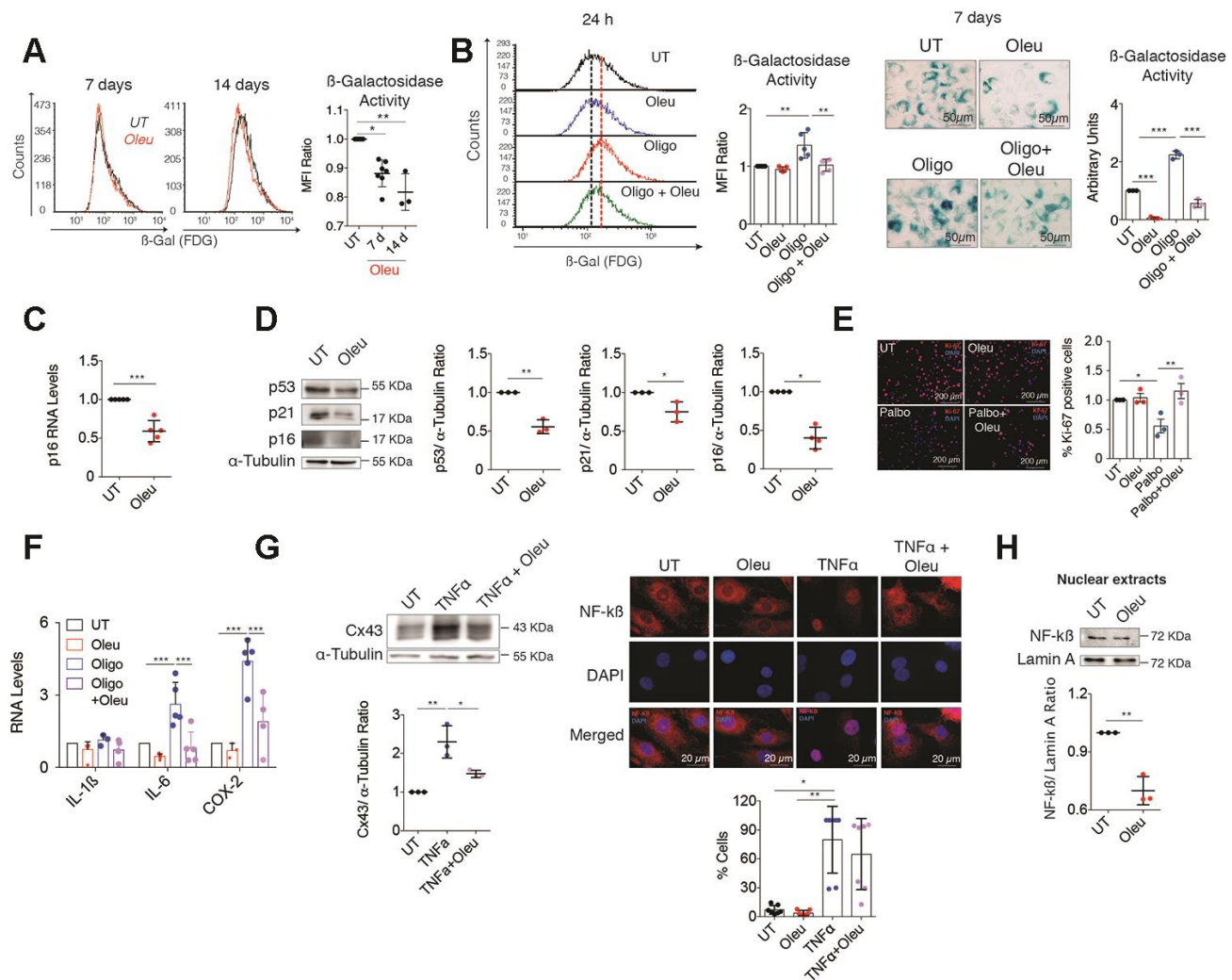

Figure 5. Cx43 downregulation by oleuropein decreased chondrocyte senescence. (**A**) SA-βGal activity detected by flow cytometry in OACs treated with 10 µM oleuropein (Oleu) for 7 and 14 days (n=3–7 independent experiments; one-way ANOVA, *P*<0.0001). (**B**) The graphs show the comparative analysis of SA-βGal activity measured by flow cytometry of OACs exposed for 24 h to 10 µM oleuropein or 5 µg/ml oligomycin as indicated (n=5 independent experiments; one-way ANOVA, *P*=0.0003). On the right, SA-βGal activity determined by X-Gal cleavage and cell staining (blue), evaluated by microscopy in OACs treated for 7 days with 10 µM oleuropein or 5 µg/ml oligomycin (n=3 independent experiments; one-way ANOVA, *P*<0.0001). (**C**) p16 mRNA expression of OACs treated with 10 µM oleuropein for 2 h. Data were normalized to HPRT-1 levels (n=5 independent experiments; Student's *t* test, *P*=0.0002). (**D**) Western blot of p53 (n=3 independent experiments), p21 (n=3 independent experiments) and p16 (n=4 independent experiments) in OACs treated with 10 µM oleuropein for 2 h. α-tubulin was used as a loading control. Student's *t* test, *P*=0.001 (p53), *P*=0.0278 (p21), *P*=0.0286 (p16). (**E**) Cell proliferation evaluated by immunofluorescence of Ki-67 in T/C-28a2 chondrocytes treated with 10 µM palbociclib and/or 10 µM oleuropein for 24 h. Images represent n= 3 independent experiments. One-way ANOVA, *P*=0.0434 (UT vs Palbo); *P*=0.0096 (Palbo vs Palbo+Oleu). (**F**) Downregulation of Cx43 by oleuropein attenuates IL-6 and COX-2 upregulation when OACs are exposed to oligomycin for 1 h (n=3–9 independent experiments; one-way ANOVA). (**G**) Western blot (n=3 independent experiments) shows the effect of 10 µM oleuropein and 10 ng/mL TNFα treatments (for 1 h) on Cx43 protein levels in OACs (one-way ANOVA, *P*=0.0018). On the right, NF-κB detected by immunofluorescence in OACs treated with 10 ng/mL TNFα for 1 h. This effect is partially abolished by 1-h 10 µM oleuropein treatment. The graph represents the cell percentage with nuclear NF-κB staining (n=7 independent experiments; one-way ANOVA, *P*=0.0055). (**H**) Nuclear levels of NF-kß in OACs cultured with 10 µM oleuropein for 2 h. Lamin A was used as a loading control (n=3 independent experiments; Student's *t* test, *P*=0.0021). Data is expressed as mean±SD; **P<0.05, ****P<0.01 and ******P<0.0001.

regeneration and fibrosis with loss of tissue function [87] (Figure 7). Understanding and manipulating the complex Cx43 signaling would expand our opportunities for modulating wound-healing related disorders such as OA. So far, our results indicate that molecules that reduce Cx43 levels in OA, including oleuropein, will potentially contribute to create a regeneration-permissive environment in OA patients.

Our preliminary study is the first to demonstrate the effect of this polyphenol on Cx43 activity and senescence. Besides, modulation of Cx43 by oleuropein

Figure 6. Oleuropein treatment decreased cellular senescence in synoviocytes and bone cells isolated from patients. (**A**) Cx43 protein levels analyzed by western blot in synoviocytes treated with 10 μM oleuropein for 2 h (n=7 independent experiments, *P*=0.0313). (**B**) Treatment of synoviocytes with 10 μM of oleuropein for 7 days detected by SA-βGal activity (n=4 independent experiments, *P*<0.0001). (**C**) p16 mRNA levels of synoviocytes treated with 10 μM oleuropein for 2 h. Data were normalized to HPRT-1 levels (n= 4 independent experiments, *P*<0.0001). On the right, mRNA levels of IL-1ß, IL-6 and COX-2 of synoviocytes cultured in normal medium (DMEM 10% FBS) and exposed to 10 μM oleuropein for 2 h. Data were normalized to HPRT-1 levels. N=4 independent experiments, *P*<0.0001 (IL-1ß), *P*=0.0024 (IL-6), *P*=0.0025 (COX-2). (**D**) Cx43 protein levels analyzed by western blot in bone cells treated with 10 μM oleuropein for 2 h (n=4 independent experiments, *P*=0.0319). (**E**) 10 μM of oleuropein treatment for 7 days reduces senescence levels in bone cells as detected by SA-βGal and flow cytometry (n=3 independent experiments, *P*=0.0149). (**F**) p16 mRNA expression of bone cells treated with 10 μM oleuropein for 2 h. Data were normalized to HPRT-1 levels (n= 4 independent experiments, *P*=0.002). On the right, mRNA levels of IL-1ß, IL-6 and COX-2 of bone cells cultured in normal medium (DMEM 10% FBS) exposed to 10 μM oleuropein for 2 h. Data were normalized to HPRT-1 levels. N=3-4 independent experiments. *P*=0.0463 (IL-1ß), *P*=0.0077 (IL-6), *P*=0.0002 (COX-2). Data is expressed as mean±SD, Student's *t* test; *P<0.05, **P<0.01 and ***P<0.0001.

shifts the hMSCs differentiation capacity towards osteogenic and chondrogenic lineages, while decreasing adipogenic differentiation. It is important to remark that aging has been reported to reduce the reparative potential of MSCs [31]. Hence, the use of small polyphenols such as oleuropein may be useful in cell therapy approaches that aim to promote cartilage and bone regeneration, as the osteogenesis/adipogenesis switch has been associated with different bone disorders [88, 89]. Altogether, these findings indicate that oleuropein controls Cx43 gene expression and acts as a senolytic drug that may serve as a potential agent to improve both the effectiveness of stem cell therapy and cartilage and joint regeneration in patients to stop OA progression. Thus, the implementation of therapies based on Cx43 modulators or innovative approaches based on functional foods enriched in olive extracts may improve joint functions and quality of life for OA patients by reducing senescence and inducing a pro-regenerative environment.

Context of damaged tissue: Cx43 overactivity in osteoarthritis
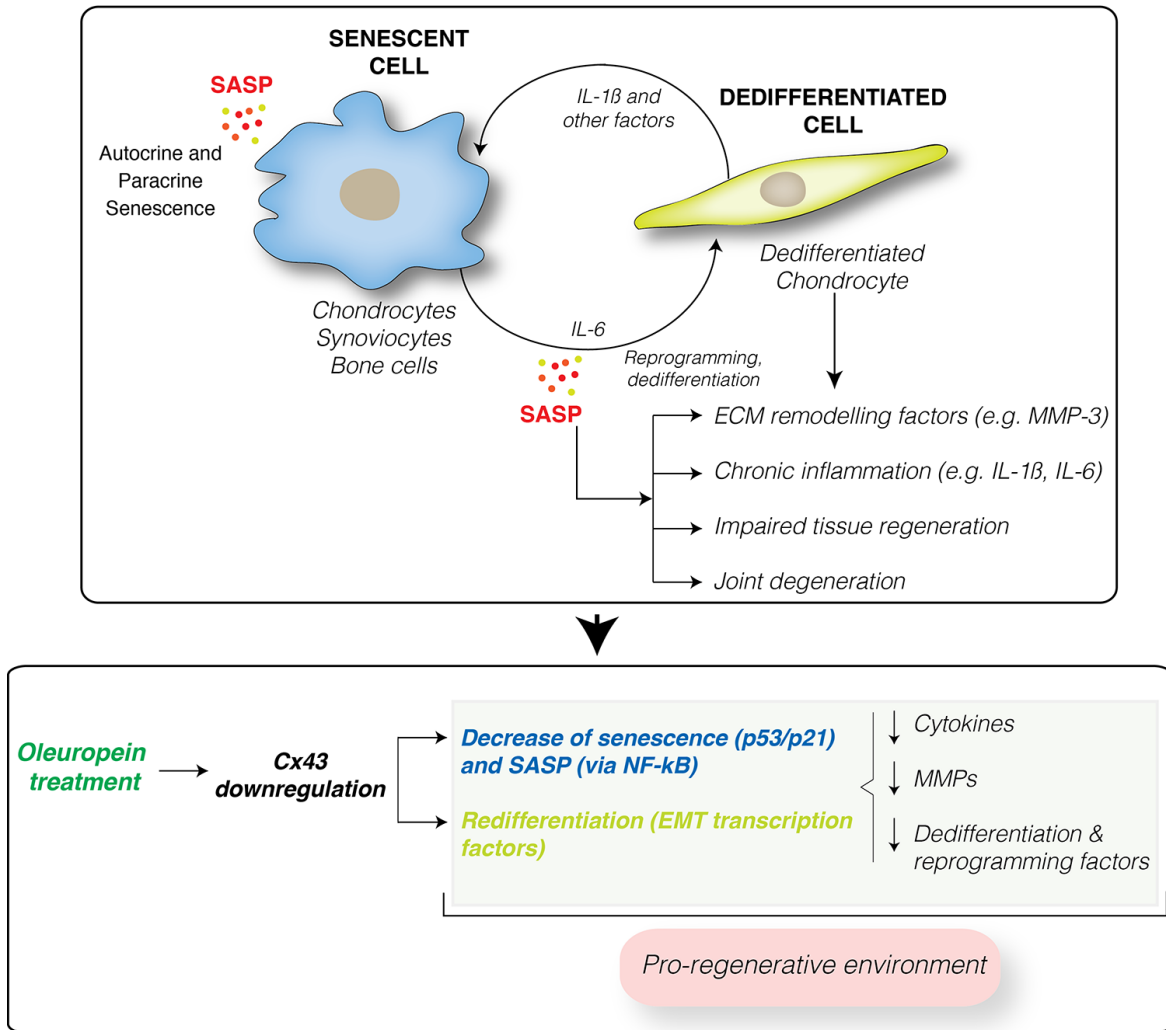

Figure 7. Cx43 overactivity contributes to disease progression. Cx43 overexpression leads to accumulation of dedifferentiated and senescent cells involved in disease progression in OA patients. These phenotypic changes results in the synthesis of ECM remodeling factors involved in tissue degradation (MMPs) and proinflammatory factors, such as IL-1ß and IL-6, which facilitate the dedifferentiation and reprogramming of neighboring cells. These factors may further spread senescence and dedifferentiation to surrounding tissues contributing to joint degeneration. Downregulation of Cx43 by oleuropein treatment contributes to the elimination of senescent cells and redifferentiation of osteoarthritic chondrocytes into fully differentiated cells, able to support the ECM composition and restoring the regenerative capacity of the tissue. However, oleuropein may have other targets that may contribute to the drug effect. In addition, oleuropein treatment might improve the effectiveness of stem cell therapy, by promoting chondrogenic and osteogenic differentiation, and by inhibiting adipogenesis.

MATERIALS AND METHODS

Tissue collection, processing and cell culture

Collection and processing of cartilage from human knees and femoral heads from adult donors undergoing joint surgery were performed as previously described [10]. Briefly, primary chondrocytes were isolated from cartilage by mechanical (dicing) and enzymatic digestion, with an incubation with 0.5 mg/mL of trypsin-EDTA (Gibco, Thermo Fisher Scientific) for 10 min at 37ºC, followed by an overnight incubation at 37ºC with a 2 mg/mL collagenase IV solution, with shaking. Finally, digested cartilage was filtered through a 100 µm strainer and chondrocytes were seeded onto 100 mm dish plates (Corning, Sigma-Aldrich). The study was conducted with the approval of the institutional ethics committee (C.0003333, 2012/094 & 2015/029) after the acquisition of signed informed consents. We have collected cartilage samples (1 sample per patient) from a total amount of 22 donors (14 OA donors and 8 healthy donors) from hip and knee joints with a mean age of 72.1±4,7 years (50% women and 50% men) within OA donors, and a mean age of 81.62±2.9 years (75% women and 25% men) within healthy donors. Cartilage samples from healthy donors were obtained after knee or hip fracture with no history of joint disease. All samples (healthy and OA) were analyzed by histological staining and classified following the American College of Rheumatology (ACR) recommendations and clinical classification criteria for OA. The chondrocyte cell line T/C-28a2 was kindly donated by Dr. Goldring (Hospital for Special Surgery; New York, USA). Primary chondrocytes and T/C-28a2 cells were cultured in Dulbecco's Modified Eagle's medium (DMEM) supplemented with 100 U/mL penicillin, 100 µg/mL streptomycin and 10% foetal bovine serum (FBS). Human mesenchymal stem cells (hMSCs) were obtained with signed informed consent from 4 bone marrow donors (*Hospital Universitario Reina Sofía*; Córdoba, Spain) and from subcutaneous inguinal fat from 2 healthy individuals (*Hospital Universitario Ramón y Cajal*; Madrid, Spain). hMSCs were cultured in MesenPRO RS^{TM} Medium supplemented with 100 U/ml penicillin and 100 µg/ml streptomycin. Synoviocytes (cultured in RPMI 10%FBS supplemented with 1% insulin-transferrin-selenium, 100 U/mL penicillin and 100 µg/mL streptomycin) and bone cells (cultured in DMEM supplemented with 100 U/mL penicillin, 100 µg/mL streptomycin and 20% inactivated FBS) from OA patients were donated by Raquel Largo (IIS-Fundación Jiménez Díaz; Madrid, Spain), after signed informed consent. hMSCs, primary chondrocytes, T/C-28a2 cells, BC and SC at 70-80% confluence were treated with oleuropein (Extrasynthese #0204; Lyon, France) or an olive extract (OE)

containing 41.5% of oleuropein, donated by the Clinical Management Unit of Endocrinology and Nutrition (IMIBIC, Córdoba, Spain). OE was dissolved in culture medium to a stock concentration equivalent to 100 µM oleuropein. Both compounds were dissolved in the cell culture medium and added to the cells for short-term (1–2 h) or long-term (7–14—21 days; each 48 hours) treatments. Bone cells and synoviocytes were treated with oleuropein 10 µM for 2 h at a 70% confluence. For cell treatments, chondrocytes at a 70-80% confluence were treated for 1 h with either 5 µg/ml oligomycin (Sigma-Aldrich) or 10 ng/mL TNFα (Immunotools). In addition, these cells were also treated simultaneously for 1 h with the combination of oligomycin or TNFα with 10 µM oleuropein. Cell proliferation arrest in T/C-28a2 healthy chondrocytes was performed by a 24h-treatment with 10 µM of Palbociclib (APExBIO) or the combination of Palbociclib and 10 µM oleuropein.

Cell viability assay

Cells at a 75% confluence were treated with 0.1 µM, 1 µM, 10 µM and 10 mM oleuropein for 17 h. Drug cytotoxicity was evaluated by the colorimetric MTT assay (Cell Proliferation Kit I, Roche) with a NanoQuant microplate reader (Tecan Trading AG) at 570 nm.

Adipogenic differentiation

Adipogenic differentiation was performed as previously described [2]. Cells were incubated with adipogenic medium (hMSC Adipogenic Differentiation Bullekit^{TM}, Lonza) for 21 days, with the addition of oleuropein or OE. Adipogenic differentiation was evaluated by the RNA expression of PPARγ and by oil red O staining.

Osteogenic differentiation

For osteogenic differentiation, cells were differentiated for 21 days with osteogenic medium (StemPro® Osteogenesis Differentiation Kit, Gibco, Thermo Fisher Scientific), with the addition of oleuropein or OE. Osteogenesis was evaluated by the RNA expression of OSTCN and by alizarin red S staining.

Chondrogenic differentiation

Chondrogenesis was performed in OACs and hMSCs as cell micromasses (3D) or as a monolayer culture. For the 3D culture, 500000 cells were seeded in non-adherent conic tubes and centrifuged at 500 x*g* for 10 min, resulting in a pellet formation, and cultured in chondrogenic medium (CM; StemPro® Chondrogenesis Differentiation Kit, Gibco, Thermo Fisher Scientific) supplemented with oleuropein or OE for 30 days. For the monolayer culture,

cells were differentiated in CM for 7/14 days with oleuropein/OE addition. Chondrogenesis was evaluated by proteoglycans detection (toluidine blue staining), Col2A1 immunohistochemistry and by ACAN mRNA expression.

Scrape loading/dye transfer (SL/DT) assay

Confluent cells were treated with oleuropein or OE for 2 h. Next, a 0.4% (w/v) solution of lucifer yellow (LY) (Cell Projects Ltd©) was loaded and two distant scrapes were made across the culture plate. In order to evaluate GJIC, a score was calculated as the ratio of non-damage positive cells for LY to the damaged cells [2, 10].

GJ connectivity by flow cytometry

Equal numbers of cells were incubated for 1 h at 37 ºC with either 1 µM of the membrane dye DiI (Invitrogen, Thermo Fisher Scientific) or 1 µM calcein-AM (Invitrogen, Thermo Fisher Scientific), a cell-permeable dye that is retained in the cytosol and can be transferred by GJs. Then, cells were washed with PBS and co-cultured for 2 h in a 1:4 ratio (calcein-donors:DiI-recipient cells). The percentage of DiI$^+$Calc$^+$ cells was analysed by flow cytometry.

Western blot

Protein analysis was performed as previously described [2, 10]. The following primary antibodies were used: α-tubulin (Sigma-Aldrich, T9026), Cx43 (Sigma-Aldrich, C6219), Twist-1 (Santa Cruz Biotechnology, sc-81417), CD166 (Santa Cruz Biotechnology, sc-74558), p16^{INK4A} (Abcam, ab108349), p21 (Santa Cruz Biotechnology, sc-6246), p53 (Santa Cruz Biotechnology, sc-126), NF-κB (Santa Cruz Biotechnology, sc-8008), lamin A (Santa Cruz Biotechnology, sc-20680), IL-6 (Sigma-Aldrich, SAB1403971) and COX-2 (Santa Cruz Biotechnology, sc-166475).

Enzyme-linked immunosorbent assay (ELISA)

Supernatants were collected after a 72 h-treatment with oleuropein 10 µM, and diluted in a 1:8 ratio prior to the measurement. Samples were incubated for 2 h at room temperature, and IL-6 was detected using the quantitative sandwich human IL-6 immunoassay (hIL-6-EIA-20, MagTag GmbH). Samples were analyzed at 450 nm in a TECAN plate reader.

Antigen expression analysis by flow cytometry

Paraformaldehyde-fixed cells were incubated with phycoerythrin (PE)-conjugated anti-human CD105 (Immunostep, 105PE-100T) or allophycocyanin (APC)-conjugated anti-human CD166 (Immunostep, 1399990314), for 30 min at 4°C, as previously reported [2] (Supplementary Table 1). Intracellular Cx43 protein was detected in paraformaldehyde-fixed cells after permeabilization with methanol for 30 min at 4ºC. Finally, cells were incubated with APC-conjugated anti-human Cx43 antibody (R&D Systems, FAB7737A) for 30 min at 4°C.

Flow cytometry analysis

20.000 events were collected on a FACSCalibur^{TM} (Becton Dickinson) flow cytometer with the CellQuest^{TM} Pro software. Cell debris was discriminated by the forward scatter (FSC) and side scatter (SSC) properties of the cells. Data were analyzed with FCS Express 6 Flow software (De Novo Software). The level of positive staining was expressed as the median fluorescence intensity (MFI), with unlabelled cells as negative controls. Gates were placed based on single-labelled controls and by establishing 0.1% as the cut-off point.

Senescence-associated β-galactosidase activity

Flow cytometry analysis of SA-βGal activity with the fluorogenic β-galactosidase substrate fluorescein di-β-D-galactopyranoside (FDG; Invitrogen, Thermo Fisher Scientific) was performed as previously described [2]. Briefly, cells were harvested and incubated with pre-warmed 2 mM FDG for 3 min at 37 ºC and fluorescein positivity was analyzed on a BD FACSCalibur^{TM} (Becton Dickinson) flow cytometer. SA-βGal activity was also measured with the Senescence Cells Histochemical Staining Kit (Sigma-Aldrich) according to the manufacturer's protocol and analyzed after 16 h of staining.

Immunofluorescence and immunohistochemistry

Immunofluorescence and immunohistochemistry assays were performed as previously described [2, 10]. The following primary antibodies were used: anti-Cx43 (Sigma-Aldrich, C6129), anti-collagen II (Invitrogen, Thermo Fisher Scientific, MA5-12789), anti-Ki-67 (BD, 550609), anti-Twist-1 (sc-81417) and anti-NF-κB (sc-8008) from Santa Cruz Biotechnology. Goat anti-rabbit FITC-conjugated (F-2765, Invitrogen, Thermo Fisher Scientific) and goat anti-mouse Alexa 594-conjugated (A-11032, Invitrogen, Thermo Fisher Scientific) secondary antibodies were used.

Quantitative PCR

TRIzol^{TM} reagent (Invitrogen, Thermo Fisher Scientific) was used to isolate total RNA, according to the manufacturer's instructions. 1 µg of total RNA per

reaction was used to synthesize cDNA with the SuperScript® VILO™ cDNA Synthesis Kit (Invitrogen, Thermo Fisher Scientific). Quantitative PCR was performed as previously described [2, 10]. Primers are listed in Supplementary Table 2.

Cell transfection

Cx43 was overexpressed, as previously described [2], in the T/C-28a2 chondrocyte cell after transfection with a pIRESpuro2 plasmid construct (Clontech) containing the human Cx43 sequence, kindly provided by Arantxa Tabernero (INCL, University of Salamanca, Spain). Electroporation was performed with the Amaxa® Cell Line Nucleofector® Kit V (Lonza) in a Nucleofector™ 2b device (Lonza) following the manufacturer's instructions.

Luciferase reporter assay

A DNA construct containing the upstream 300 bp-regulatory sequence of the human Cx43 promoter (–108, +279, relative to the human Cx43 transcription start site) in a pGL3-Basic vector was kindly donated by Dr. Mustapha Kandouz (Wayne State University, USA). The T/C-28a2 chondrocyte cell line was transfected with the Amaxa® Cell Line Nucleofector® Kit V in a Nucleofector™ 2b device. After 24 h, cells were treated with 10 µM oleuropein and/or 5 µg/ml of oligomycin (Sigma-Aldrich) for 1 h. For the luminescence analysis, the Firefly Luciferase Assay Kit from Biotium was used according to the manufacturer's instructions, and normalized to the total protein content.

Statistical analysis

Statistical analysis was performed with GraphPad Prism software (version 7.0a). Data of the biological and/or technical replicates are represented as mean and SD. Two-tailed Unpaired Student's t test was used to estimate statistically significant differences between two groups. The estimation of the difference of the means among groups was compared by one-way ANOVA with Bonferroni correction. P values were provided, with $P<0.05$ considered as statistically significant. *$P<0.05$, **$P<0.01$ and ***$P<0.0001$.

Abbreviations

ACAN: aggrecan; AM: adipogenic medium; BC: bone cells; CBX: carbenoxolone; CD105: endoglin; CD166: CD166 antigen (ALCAM); CM: chondrogenic medium; CMT: chondrocyte-to-mesenchymal transition; Col2A1: collagen type II; COX-2: cyclooxygenase-2; Cx43: connexin43; CxREs: connexin-response elements; ECM: extracellular matrix; EMT: epithelial-to-mesenchymal transition; FDG: fluorescein-di-D-galactopyranoside; GJs: gap junctions; GJIC: gap junction intercellular communication; hMSCs: human mesenchymal stem cells; IL-1β: interleukin 1 beta; IL-6: interleukin 6; LY: Lucifer yellow; MMP-3: matrix metalloproteinase 3; NF-κB: nuclear factor kappa-light-chain-enhancer of activated B cells; OA: osteoarthritis; OACs: osteoarthritic chondrocytes; OE: olive extract; OM: osteogenic medium; Oleu: Oleuropein; OSTCN: osteocalcin; p16: cyclin-dependent kinase inhibitor 2A; p53: cellular tumour antigen p53; PPARγ: peroxisome proliferator-activated receptor gamma; RT-qPCR: real-time quantitative polymerase chain reaction; SA-βGal: senescence-associated β-galactosidase activity; SASP: senescence-associated secretory phenotype; SC: synovial cells; TNFα: tumour necrosis factor alpha; Twist-1: twist-related protein 1.

AUTHOR CONTRIBUTIONS

ACKNOWLEDGMENTS

CONFLICTS OF INTEREST

FUNDING

REFERENCES

1. Jeon OH, Kim C, Laberge RM, Demaria M, Rathod S, Vasserot AP, Chung JW, Kim DH, Poon Y, David N, Baker DJ, van Deursen JM, Campisi J, Elisseeff JH. Local clearance of senescent cells attenuates the development of post-traumatic osteoarthritis and creates a pro-regenerative environment. Nat Med. 2017; 23:775–81.
https://doi.org/10.1038/nm.4324 PMID:28436958

2. Varela-Eirín M, Varela-Vázquez A, Guitián-Caamaño A, Paíno CL, Mato V, Largo R, Aasen T, Tabernero A, Fonseca E, Kandouz M, Caeiro JR, Blanco A, Mayán MD. Targeting of chondrocyte plasticity via connexin43 modulation attenuates cellular senescence and fosters a pro-regenerative environment in osteoarthritis. Cell Death Dis. 2018; 9:1166.
https://doi.org/10.1038/s41419-018-1225-2 PMID:30518918

3. Alsalameh S, Amin R, Gemba T, Lotz M. Identification of mesenchymal progenitor cells in normal and osteoarthritic human articular cartilage. Arthritis Rheum. 2004; 50:1522–32.
https://doi.org/10.1002/art.20269 PMID:15146422

4. Grogan SP, Miyaki S, Asahara H, D'Lima DD, Lotz MK. Mesenchymal progenitor cell markers in human articular cartilage: normal distribution and changes in osteoarthritis. Arthritis Res Ther. 2009; 11:R85.
https://doi.org/10.1186/ar2719 PMID:19500336

5. Goldring MB, Marcu KB. Cartilage homeostasis in health and rheumatic diseases. Arthritis Res Ther. 2009; 11:224.
https://doi.org/10.1186/ar2592 PMID:19519926

6. Montgomery J, Ghatnekar GS, Grek CL, Moyer KE, Gourdie RG. Connexin 43-based therapeutics for dermal wound healing. Int J Mol Sci. 2018; 19:1778.
https://doi.org/10.3390/ijms19061778 PMID:29914066

7. Aasen T, Leithe E, Graham SV, Kameritsch P, Mayán MD, Mesnil M, Pogoda K, Tabernero A. Connexins in cancer: bridging the gap to the clinic. Oncogene. 2019; 38:4429–51.
https://doi.org/10.1038/s41388-019-0741-6 PMID:30814684

8. Gago-Fuentes R, Fernández-Puente P, Megias D, Carpintero-Fernández P, Mateos J, Acea B, Fonseca E, Blanco FJ, Mayan MD. Proteomic analysis of connexin 43 reveals novel interactors related to osteoarthritis. Mol Cell Proteomics. 2015; 14:1831–45.
https://doi.org/10.1074/mcp.M115.050211 PMID:25903580

9. Mayan MD, Carpintero-Fernandez P, Gago-Fuentes R, Martinez-de-Ilarduya O, Wang HZ, Valiunas V, Brink P, Blanco FJ. Human articular chondrocytes express multiple gap junction proteins: differential expression of connexins in normal and osteoarthritic cartilage. Am J Pathol. 2013; 182:1337–46.
https://doi.org/10.1016/j.ajpath.2012.12.018 PMID:23416160

10. Mayan MD, Gago-Fuentes R, Carpintero-Fernandez P, Fernandez-Puente P, Filgueira-Fernandez P, Goyanes N, Valiunas V, Brink PR, Goldberg GS, Blanco FJ. Articular chondrocyte network mediated by gap junctions: role in metabolic cartilage homeostasis. Ann Rheum Dis. 2015; 74:275–84.
https://doi.org/10.1136/annrheumdis-2013-204244 PMID:24225059

11. Marino AA, Waddell DD, Kolomytkin OV, Meek WD, Wolf R, Sadasivan KK, Albright JA. Increased intercellular communication through gap junctions may contribute to progression of osteoarthritis. Clin Orthop Relat Res. 2004; 422:224–32.
https://doi.org/10.1097/01.blo.0000129346.29945.3b PMID:15187861

12. Gago-Fuentes R, Bechberger JF, Varela-Eirin M, Varela-Vazquez A, Acea B, Fonseca E, Naus CC, Mayan MD. The c-terminal domain of connexin43 modulates cartilage structure via chondrocyte phenotypic changes. Oncotarget. 2016; 7:73055–67.
https://doi.org/10.18632/oncotarget.12197 PMID:27682878

13. Plotkin LI, Bellido T. Beyond gap junctions: Connexin43 and bone cell signaling. Bone. 2013; 52:157–66.
https://doi.org/10.1016/j.bone.2012.09.030 PMID:23041511

14. Tsuchida S, Arai Y, Kishida T, Takahashi KA, Honjo K, Terauchi R, Inoue H, Oda R, Mazda O, Kubo T. Silencing the expression of connexin 43 decreases inflammation and joint destruction in experimental arthritis. J Orthop Res. 2013; 31:525–30.
https://doi.org/10.1002/jor.22263 PMID:23165424

15. Gupta A, Niger C, Buo AM, Eidelman ER, Chen RJ, Stains JP. Connexin43 enhances the expression of osteoarthritis-associated genes in synovial fibroblasts in culture. BMC Musculoskelet Disord. 2014; 15:425. https://doi.org/10.1186/1471-2474-15-425 PMID:25496568

16. Gurtner GC, Werner S, Barrandon Y, Longaker MT. Wound repair and regeneration. Nature. 2008; 453:314–21. https://doi.org/10.1038/nature07039 PMID:18480812

17. Loeser RF, Collins JA, Diekman BO. Ageing and the pathogenesis of osteoarthritis. Nat Rev Rheumatol. 2016; 12:412–20. https://doi.org/10.1038/nrrheum.2016.65 PMID:27192932

18. Gao SG, Zeng C, Li LJ, Luo W, Zhang FJ, Tian J, Cheng C, Tu M, Xiong YL, Jiang W, Xu M, Lei GH. Correlation between senescence-associated beta-galactosidase expression in articular cartilage and disease severity of patients with knee osteoarthritis. Int J Rheum Dis. 2016; 19:226–32. https://doi.org/10.1111/1756-185X.12096 PMID:26112901

19. Philipot D, Guérit D, Platano D, Chuchana P, Olivotto E, Espinoza F, Dorandeu A, Pers YM, Piette J, Borzi RM, Jorgensen C, Noel D, Brondello JM. p16INK4a and its regulator miR-24 link senescence and chondrocyte terminal differentiation-associated matrix remodeling in osteoarthritis. Arthritis Res Ther. 2014; 16:R58. https://doi.org/10.1186/ar4494 PMID:24572376

20. Price JS, Waters JG, Darrah C, Pennington C, Edwards DR, Donell ST, Clark IM. The role of chondrocyte senescence in osteoarthritis. Aging Cell. 2002; 1:57–65. https://doi.org/10.1046/j.1474-9728.2002.00008.x PMID:12882354

21. Loeser RF. Aging and osteoarthritis: the role of chondrocyte senescence and aging changes in the cartilage matrix. Osteoarthritis Cartilage. 2009; 17:971–79. https://doi.org/10.1016/j.joca.2009.03.002 PMID:19303469

22. Collins JA, Diekman BO, Loeser RF. Targeting aging for disease modification in osteoarthritis. Curr Opin Rheumatol. 2018; 30:101–07. https://doi.org/10.1097/BOR.0000000000000456 PMID:28957964

23. Tchkonia T, Zhu Y, van Deursen J, Campisi J, Kirkland JL. Cellular senescence and the senescent secretory phenotype: therapeutic opportunities. J Clin Invest. 2013; 123:966–72. https://doi.org/10.1172/JCI64098 PMID:23454759

24. Peilin W, Songsong T, Chengyu Z, Zhi C, Chunhui M, Yinxian Y, Lei Z, Min M, Zongyi W, Mengkai Y, Jing X, Tao Z, Zhuoying W, et al. Directed elimination of senescent cells attenuates development of osteoarthritis by inhibition of c-IAP and XIAP. Biochim Biophys Acta Mol Basis Dis. 2019; 1865:2618–32. https://doi.org/10.1016/j.bbadis.2019.05.017 PMID:31251987

25. Nogueira-Recalde U, Lorenzo-Gómez I, Blanco FJ, Loza MI, Grassi D, Shirinsky V, Shirinsky I, Lotz M, Robbins PD, Domínguez E, Caramés B. Fibrates as drugs with senolytic and autophagic activity for osteoarthritis therapy. EBioMedicine. 2019; 45:588–605. https://doi.org/10.1016/j.ebiom.2019.06.049 PMID:31285188

26. Yang H, Chen C, Chen H, Duan X, Li J, Zhou Y, Zeng W, Yang L. Navitoclax (ABT263) reduces inflammation and promotes chondrogenic phenotype by clearing senescent osteoarthritic chondrocytes in osteoarthritis. Aging (Albany NY). 2020; 12:12750–70. https://doi.org/10.18632/aging.103177 PMID:32611834

27. Zhu Y, Doornebal EJ, Pirtskhalava T, Giorgadze N, Wentworth M, Fuhrmann-Stroissnigg H, Niedernhofer LJ, Robbins PD, Tchkonia T, Kirkland JL. New agents that target senescent cells: the flavone, fisetin, and the BCL-X$_L$ inhibitors, A1331852 and A1155463. Aging (Albany NY). 2017; 9:955–63. https://doi.org/10.18632/aging.101202 PMID:28273655

28. Zheng W, Feng Z, You S, Zhang H, Tao Z, Wang Q, Chen H, Wu Y. Fisetin inhibits IL-1β-induced inflammatory response in human osteoarthritis chondrocytes through activating SIRT1 and attenuates the progression of osteoarthritis in mice. Int Immunopharmacol. 2017; 45:135–47. https://doi.org/10.1016/j.intimp.2017.02.009 PMID:28213268

29. Cao X, Luo P, Huang J, Liang C, He J, Wang Z, Shan D, Peng C, Wu S. Intraarticular senescent chondrocytes impair the cartilage regeneration capacity of mesenchymal stem cells. Stem Cell Res Ther. 2019; 10:86. https://doi.org/10.1186/s13287-019-1193-1 PMID:30867061

30. Kang D, Shin J, Cho Y, Kim HS, Gu YR, Kim H, You KT, Chang MJ, Chang CB, Kang SB, Kim JS, Kim VN, Kim JH. Stress-activated miR-204 governs senescent phenotypes of chondrocytes to promote osteoarthritis development. Sci Transl Med. 2019; 11:eaar6659. https://doi.org/10.1126/scitranslmed.aar6659 PMID:30944169

31. Szychlinska MA, Stoddart MJ, D'Amora U, Ambrosio L, Alini M, Musumeci G. Mesenchymal stem cell-based cartilage regeneration approach and cell senescence: can we manipulate cell aging and function? Tissue Eng Part B Rev. 2017; 23:529–39.
https://doi.org/10.1089/ten.TEB.2017.0083
PMID:28514935

32. Xu M, Bradley EW, Weivoda MM, Hwang SM, Pirtskhalava T, Decklever T, Curran GL, Ogrodnik M, Jurk D, Johnson KO, Lowe V, Tchkonia T, Westendorf JJ, Kirkland JL. Transplanted senescent cells induce an osteoarthritis-like condition in mice. J Gerontol A Biol Sci Med Sci. 2017; 72:780–85.
https://doi.org/10.1093/gerona/glw154
PMID:27516624

33. Laird DW. Syndromic and non-syndromic disease-linked Cx43 mutations. FEBS Lett. 2014; 588:1339–48.
https://doi.org/10.1016/j.febslet.2013.12.022
PMID:24434540

34. Yang Y, Ren J, Sun Y, Xue Y, Zhang Z, Gong A, Wang B, Zhong Z, Cui Z, Xi Z, Yang GY, Sun Q, Bian L. A connexin43/YAP axis regulates astroglial-mesenchymal transition in hemoglobin induced astrocyte activation. Cell Death Differ. 2018; 25:1870–84.
https://doi.org/10.1038/s41418-018-0137-0
PMID:29880858

35. Varela-Eirin M, Loureiro J, Fonseca E, Corrochano S, Caeiro JR, Collado M, Mayan MD. Cartilage regeneration and ageing: targeting cellular plasticity in osteoarthritis. Ageing Res Rev. 2018; 42:56–71.
https://doi.org/10.1016/j.arr.2017.12.006
PMID:29258883

36. Casagrande D, Stains JP, Murthi AM. Identification of shoulder osteoarthritis biomarkers: comparison between shoulders with and without osteoarthritis. J Shoulder Elbow Surg. 2015; 24:382–90.
https://doi.org/10.1016/j.jse.2014.11.039
PMID:25595362

37. Tonon R, D'Andrea P. The functional expression of connexin 43 in articular chondrocytes is increased by interleukin 1beta: evidence for a Ca2+-dependent mechanism. Biorheology. 2002; 39:153–60.
PMID:12082278

38. Aigner T, Zien A, Gehrsitz A, Gebhard PM, McKenna L. Anabolic and catabolic gene expression pattern analysis in normal versus osteoarthritic cartilage using complementary DNA-array technology. Arthritis Rheum. 2001; 44:2777–89.
https://doi.org/10.1002/1529-0131(200112)44:12<2777::aid-art465>3.0.co;2-h PMID:11762938

39. Koelling S, Kruegel J, Irmer M, Path JR, Sadowski B, Miro X, Miosge N. Migratory chondrogenic progenitor cells from repair tissue during the later stages of human osteoarthritis. Cell Stem Cell. 2009; 4:324–35.
https://doi.org/10.1016/j.stem.2009.01.015
PMID:19341622

40. Kim AC, Spector M. Distribution of chondrocytes containing alpha-smooth muscle actin in human articular cartilage. J Orthop Res. 2000; 18:749–55.
https://doi.org/10.1002/jor.1100180511
PMID:11117296

41. Dowthwaite GP, Bishop JC, Redman SN, Khan IM, Rooney P, Evans DJ, Haughton L, Bayram Z, Boyer S, Thomson B, Wolfe MS, Archer CW. The surface of articular cartilage contains a progenitor cell population. J Cell Sci. 2004; 117:889–97.
https://doi.org/10.1242/jcs.00912 PMID:14762107

42. Fickert S, Fiedler J, Brenner RE. Identification of subpopulations with characteristics of mesenchymal progenitor cells from human osteoarthritic cartilage using triple staining for cell surface markers. Arthritis Res Ther. 2004; 6:R422–32.
https://doi.org/10.1186/ar1210 PMID:15380042

43. Jiang Y, Cai Y, Zhang W, Yin Z, Hu C, Tong T, Lu P, Zhang S, Neculai D, Tuan RS, Ouyang HW. Human cartilage-derived progenitor cells from committed chondrocytes for efficient cartilage repair and regeneration. Stem Cells Transl Med. 2016; 5:733–44.
https://doi.org/10.5966/sctm.2015-0192
PMID:27130221

44. Li L, Newton PT, Bouderlique T, Sejnohova M, Zikmund T, Kozhemyakina E, Xie M, Krivanek J, Kaiser J, Qian H, Dyachuk V, Lassar AB, Warman ML, et al. Superficial cells are self-renewing chondrocyte progenitors, which form the articular cartilage in juvenile mice. FASEB J. 2017; 31:1067–84.
https://doi.org/10.1096/fj.201600918R
PMID:27965322

45. Mori R, Power KT, Wang CM, Martin P, Becker DL. Acute downregulation of connexin43 at wound sites leads to a reduced inflammatory response, enhanced keratinocyte proliferation and wound fibroblast migration. J Cell Sci. 2006; 119:5193–203.
https://doi.org/10.1242/jcs.03320 PMID:17158921

46. Pollok S, Pfeiffer AC, Lobmann R, Wright CS, Moll I, Martin PE, Brandner JM. Connexin 43 mimetic peptide Gap27 reveals potential differences in the role of Cx43 in wound repair between diabetic and non-diabetic cells. J Cell Mol Med. 2011; 15:861–73.
https://doi.org/10.1111/j.1582-4934.2010.01057.x
PMID:20345849

47. Ongstad EL, O'Quinn MP, Ghatnekar GS, Yost MJ, Gourdie RG. A Connexin43 mimetic peptide promotes regenerative healing and improves mechanical
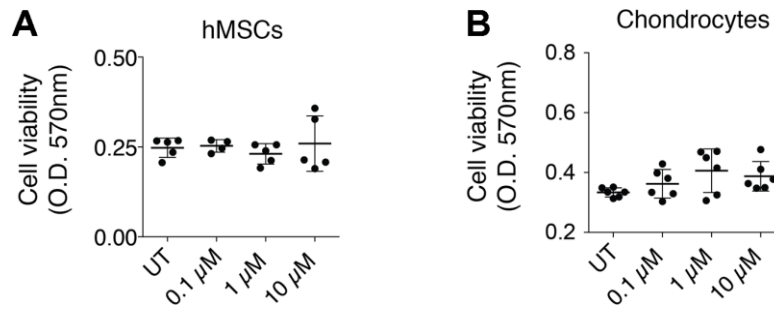
properties in skin and heart. Adv Wound Care (New Rochelle). 2013; 2:55–62.
https://doi.org/10.1089/wound.2011.0341
PMID:24527326

48. Omar SH. Oleuropein in olive and its pharmacological effects. Sci Pharm. 2010; 78:133–54.
https://doi.org/10.3797/scipharm.0912-18
PMID:21179340

49. Corominas-Faja B, Santangelo E, Cuyàs E, Micol V, Joven J, Ariza X, Segura-Carretero A, García J, Menendez JA. Computer-aided discovery of biological activity spectra for anti-aging and anti-cancer olive oil oleuropeins. Aging (Albany NY). 2014; 6:731–41.
https://doi.org/10.18632/aging.100691
PMID:25324469

50. Sarsour EH, Kumar MG, Kalen AL, Goswami M, Buettner GR, Goswami PC. MnSOD activity regulates hydroxytyrosol-induced extension of chronological lifespan. Age (Dordr). 2012; 34:95–109.
https://doi.org/10.1007/s11357-011-9223-7
PMID:21384152

51. Omar SH. Cardioprotective and neuroprotective roles of oleuropein in olive. Saudi Pharm J. 2010; 18:111–21.
https://doi.org/10.1016/j.jsps.2010.05.005
PMID:23964170

52. St-Laurent-Thibault C, Arseneault M, Longpré F, Ramassamy C. Tyrosol and hydroxytyrosol, two main components of olive oil, protect N2a cells against amyloid-β-induced toxicity. Involvement of the NF-κB signaling. Curr Alzheimer Res. 2011; 8:543–51.
https://doi.org/10.2174/156720511796391845
PMID:21605049

53. Yonezawa Y, Miyashita T, Nejishima H, Takeda Y, Imai K, Ogawa H. Anti-inflammatory effects of olive-derived hydroxytyrosol on lipopolysaccharide-induced inflammation in RAW264.7 cells. J Vet Med Sci. 2018; 80:1801–07.
https://doi.org/10.1292/jvms.18-0250 PMID:30298817

54. Wang W, Shang C, Zhang W, Jin Z, Yao F, He Y, Wang B, Li Y, Zhang J, Lin R. Hydroxytyrosol NO regulates oxidative stress and NO production through SIRT1 in diabetic mice and vascular endothelial cells. Phytomedicine. 2019; 52:206–15.
https://doi.org/10.1016/j.phymed.2018.09.208
PMID:30599900

55. Rigacci S, Miceli C, Nediani C, Berti A, Cascella R, Pantano D, Nardiello P, Luccarini I, Casamenti F, Stefani M. Oleuropein aglycone induces autophagy via the AMPK/mTOR signalling pathway: a mechanistic insight. Oncotarget. 2015; 6:35344–57.
https://doi.org/10.18632/oncotarget.6119
PMID:26474288

56. Cetrullo S, D'Adamo S, Guidotti S, Borzì RM, Flamigni F. Hydroxytyrosol prevents chondrocyte death under oxidative stress by inducing autophagy through sirtuin 1-dependent and -independent mechanisms. Biochim Biophys Acta. 2016; 1860:1181–91.
https://doi.org/10.1016/j.bbagen.2016.03.002
PMID:26947008

57. Kim Y, Choi Y, Park T. Hepatoprotective effect of oleuropein in mice: mechanisms uncovered by gene expression profiling. Biotechnol J. 2010; 5:950–60.
https://doi.org/10.1002/biot.201000068
PMID:20845385

58. Farràs M, Arranz S, Carrión S, Subirana I, Muñoz-Aguayo D, Blanchart G, Kool M, Solà R, Motilva MJ, Escolà-Gil JC, Rubió L, Fernández-Castillejo S, Pedret A, et al. A functional virgin olive oil enriched with olive oil and thyme phenolic compounds improves the expression of cholesterol efflux-related genes: a randomized, crossover, controlled trial. Nutrients. 2019; 11:1732.
https://doi.org/10.3390/nu11081732 PMID:31357534

59. de Pablos RM, Espinosa-Oliva AM, Hornedo-Ortega R, Cano M, Arguelles S. Hydroxytyrosol protects from aging process via AMPK and autophagy; a review of its effects on cancer, metabolic syndrome, osteoporosis, immune-mediated and neurodegenerative diseases. Pharmacol Res. 2019; 143:58–72.
https://doi.org/10.1016/j.phrs.2019.03.005
PMID:30853597

60. Battino M, Forbes-Hernández TY, Gasparrini M, Afrin S, Cianciosi D, Zhang J, Manna PP, Reboredo-Rodríguez P, Varela Lopez A, Quiles JL, Mezzetti B, Bompadre S, Xiao J, Giampieri F. Relevance of functional foods in the mediterranean diet: the role of olive oil, berries and honey in the prevention of cancer and cardiovascular diseases. Crit Rev Food Sci Nutr. 2019; 59:893–920.
https://doi.org/10.1080/10408398.2018.1526165
PMID:30421983

61. Casamenti F, Stefani M. Olive polyphenols: new promising agents to combat aging-associated neurodegeneration. Expert Rev Neurother. 2017; 17:345–58.
https://doi.org/10.1080/14737175.2017.1245617
PMID:27762153

62. García-Gavilán JF, Bulló M, Canudas S, Martínez-González MA, Estruch R, Giardina S, Fitó M, Corella D, Ros E, Salas-Salvadó J. Extra virgin olive oil consumption reduces the risk of osteoporotic fractures in the PREDIMED trial. Clin Nutr. 2018; 37:329–35.
https://doi.org/10.1016/j.clnu.2016.12.030
PMID:28143667

63. Musumeci G, Trovato FM, Pichler K, Weinberg AM, Loreto C, Castrogiovanni P. Extra-virgin olive oil diet

and mild physical activity prevent cartilage degeneration in an osteoarthritis model: an in vivo and in vitro study on lubricin expression. J Nutr Biochem. 2013; 24:2064–75.
https://doi.org/10.1016/j.jnutbio.2013.07.007
PMID:24369033

64. Szychlinska MA, Castrogiovanni P, Trovato FM, Nsir H, Zarrouk M, Lo Furno D, Di Rosa M, Imbesi R, Musumeci G. Physical activity and mediterranean diet based on olive tree phenolic compounds from two different geographical areas have protective effects on early osteoarthritis, muscle atrophy and hepatic steatosis. Eur J Nutr. 2019; 58:565–81.
https://doi.org/10.1007/s00394-018-1632-2
PMID:29450729

65. Bohlooli S, Jastan M, Nakhostin-Roohi B, Mohammadi S, Baghaei Z. A pilot double-blinded, randomized, clinical trial of topical virgin olive oil versus piroxicam gel in osteoarthritis of the knee. J Clin Rheumatol. 2012; 18:99–101.
https://doi.org/10.1097/RHU.0b013e31824a47b5
PMID:22334264

66. Scotece M, Conde J, Abella V, López V, Francisco V, Ruiz C, Campos V, Lago F, Gomez R, Pino J, Gualillo O. Oleocanthal inhibits catabolic and inflammatory mediators in LPS-activated human primary osteoarthritis (OA) chondrocytes through MAPKs/NF-κB pathways. Cell Physiol Biochem. 2018; 49:2414–26.
https://doi.org/10.1159/000493840
PMID:30261513

67. Chin KY, Pang KL. Therapeutic effects of olive and its derivatives on osteoarthritis: from bench to bedside. Nutrients. 2017; 9:1060.
https://doi.org/10.3390/nu9101060 PMID:28954409

68. Musumeci G, Castrogiovanni P, Trovato FM, Imbesi R, Giunta S, Szychlinska MA, Loreto C, Castorina S, Mobasheri A. Physical activity ameliorates cartilage degeneration in a rat model of aging: a study on lubricin expression. Scand J Med Sci Sports. 2015; 25:e222–30.
https://doi.org/10.1111/sms.12290 PMID:25039883

69. Santiago-Mora R, Casado-Díaz A, De Castro MD, Quesada-Gómez JM. Oleuropein enhances osteoblastogenesis and inhibits adipogenesis: the effect on differentiation in stem cells derived from bone marrow. Osteoporos Int. 2011; 22:675–84.
https://doi.org/10.1007/s00198-010-1270-x
PMID:20495905

70. Tian H. Detection of differentially expressed genes involved in osteoarthritis pathology. J Orthop Surg Res. 2018; 13:49.
https://doi.org/10.1186/s13018-018-0734-0
PMID:29514675

71. Karlsson C, Dehne T, Lindahl A, Brittberg M, Pruss A, Sittinger M, Ringe J. Genome-wide expression profiling reveals new candidate genes associated with osteoarthritis. Osteoarthritis Cartilage. 2010; 18:581–92.
https://doi.org/10.1016/j.joca.2009.12.002
PMID:20060954

72. Mayan MD, Blanco FJ, Carpintero-Fernandez P and Goldberg GS. (2 July 2014). Compositions and Methods to Treat Inflammatory Joint Diseases. United States Patent Application 20160375096.

73. Carpintero-Fernandez P, Varela-Eirin M, Lacetera A, Gago-Fuentes R, Fonseca E, Martin-Santamaria S, Mayan MD. New therapeutic strategies for osteoarthritis by targeting sialic acid receptors. Biomolecules. 2020; 10:637.
https://doi.org/10.3390/biom10040637
PMID:32326143

74. Mosteiro L, Pantoja C, Alcazar N, Marión RM, Chondronasiou D, Rovira M, Fernandez-Marcos PJ, Muñoz-Martin M, Blanco-Aparicio C, Pastor J, Gómez-López G, De Martino A, Blasco MA, et al. Tissue damage and senescence provide critical signals for cellular reprogramming in vivo. Science. 2016; 354:aaf4445.
https://doi.org/10.1126/science.aaf4445
PMID:27884981

75. Chien Y, Scuoppo C, Wang X, Fang X, Balgley B, Bolden JE, Premsrirut P, Luo W, Chicas A, Lee CS, Kogan SC, Lowe SW. Control of the senescence-associated secretory phenotype by NF-κB promotes senescence and enhances chemosensitivity. Genes Dev. 2011; 25:2125–36.
https://doi.org/10.1101/gad.17276711
PMID:21979375

76. Feng Z, Li X, Lin J, Zheng W, Hu Z, Xuan J, Ni W, Pan X. Oleuropein inhibits the IL-1β-induced expression of inflammatory mediators by suppressing the activation of NF-κB and MAPKs in human osteoarthritis chondrocytes. Food Funct. 2017; 8:3737–44.
https://doi.org/10.1039/c7fo00823f PMID:28952621

77. Horcajada MN, Sanchez C, Membrez Scalfo F, Drion P, Comblain F, Taralla S, Donneau AF, Offord EA, Henrotin Y. Oleuropein or rutin consumption decreases the spontaneous development of osteoarthritis in the hartley Guinea pig. Osteoarthritis Cartilage. 2015; 23:94–102.
https://doi.org/10.1016/j.joca.2014.08.016
PMID:25219641

78. Bulotta S, Celano M, Lepore SM, Montalcini T, Pujia A, Russo D. Beneficial effects of the olive oil phenolic components oleuropein and hydroxytyrosol: focus on protection against cardiovascular and metabolic
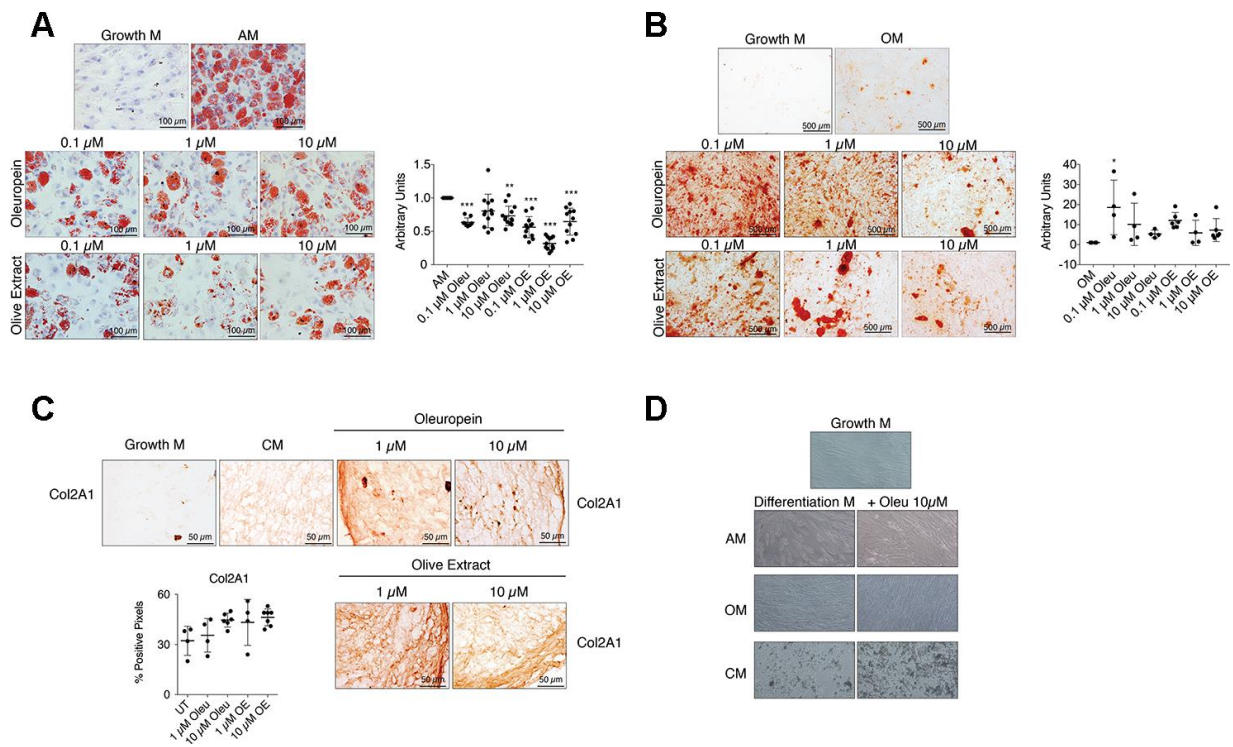
diseases. J Transl Med. 2014; 12:219.
https://doi.org/10.1186/s12967-014-0219-9
PMID:25086598

79. Solan JL, Lampe PD. Spatio-temporal regulation of connexin43 phosphorylation and gap junction dynamics. Biochim Biophys Acta Biomembr. 2018; 1860:83–90.
https://doi.org/10.1016/j.bbamem.2017.04.008
PMID:28414037

80. Spagnol G, Trease AJ, Zheng L, Gutierrez M, Basu I, Sarmiento C, Moore G, Cervantes M, Sorgen PL. Connexin43 carboxyl-terminal domain directly interacts with β-catenin. Int J Mol Sci. 2018; 19:1562.
https://doi.org/10.3390/ijms19061562
PMID:29882937

81. González-Sánchez A, Jaraíz-Rodríguez M, Domínguez-Prieto M, Herrero-González S, Medina JM, Tabernero A. Connexin43 recruits PTEN and csk to inhibit c-src activity in glioma cells and astrocytes. Oncotarget. 2016; 7:49819–33.
https://doi.org/10.18632/oncotarget.10454
PMID:27391443

82. Kotini M, Barriga EH, Leslie J, Gentzel M, Rauschenberger V, Schambony A, Mayor R. Gap junction protein connexin-43 is a direct transcriptional regulator of n-cadherin in vivo. Nat Commun. 2018; 9:3846.
https://doi.org/10.1038/s41467-018-06368-x
PMID:30242148

83. Acosta JC, O'Loghlen A, Banito A, Guijarro MV, Augert A, Raguz S, Fumagalli M, Da Costa M, Brown C, Popov N, Takatsu Y, Melamed J, d'Adda di Fagagna F, et al. Chemokine signaling via the CXCR2 receptor reinforces senescence. Cell. 2008; 133:1006–18.
https://doi.org/10.1016/j.cell.2008.03.038
PMID:18555777

84. Ferrand M, Kirsh O, Griveau A, Vindrieux D, Martin N, Defossez PA, Bernard D. Screening of a kinase library reveals novel pro-senescence kinases and their common NF-κB-dependent transcriptional program. Aging (Albany NY). 2015; 7:986–1003.

https://doi.org/10.18632/aging.100845
PMID:26583757

85. Demaria M, Ohtani N, Youssef SA, Rodier F, Toussaint W, Mitchell JR, Laberge RM, Vijg J, Van Steeg H, Dollé ME, Hoeijmakers JH, de Bruin A, Hara E, Campisi J. An essential role for senescent cells in optimal wound healing through secretion of PDGF-AA. Dev Cell. 2014; 31:722–33.
https://doi.org/10.1016/j.devcel.2014.11.012
PMID:25499914

86. Vazquez-Martin A, Van den Haute C, Cufí S, Corominas-Faja B, Cuyàs E, Lopez-Bonet E, Rodriguez-Gallego E, Fernández-Arroyo S, Joven J, Baekelandt V, Menendez JA. Mitophagy-driven mitochondrial rejuvenation regulates stem cell fate. Aging (Albany NY). 2016; 8:1330–52.
https://doi.org/10.18632/aging.100976
PMID:27295498

87. Muñoz-Espín D, Serrano M. Cellular senescence: from physiology to pathology. Nat Rev Mol Cell Biol. 2014; 15:482–96.
https://doi.org/10.1038/nrm3823
PMID:24954210

88. Li CJ, Cheng P, Liang MK, Chen YS, Lu Q, Wang JY, Xia ZY, Zhou HD, Cao X, Xie H, Liao EY, Luo XH. MicroRNA-188 regulates age-related switch between osteoblast and adipocyte differentiation. J Clin Invest. 2015; 125:1509–22.
https://doi.org/10.1172/JCI77716
PMID:25751060

89. Guo J, Ren R, Yao X, Ye Y, Sun K, Lin J, Wang G, Guo F, Xiao J, Xu T. PKM2 suppresses osteogenesis and facilitates adipogenesis by regulating β-catenin signaling and mitochondrial fusion and fission. Aging (Albany NY). 2020; 12:3976–92.
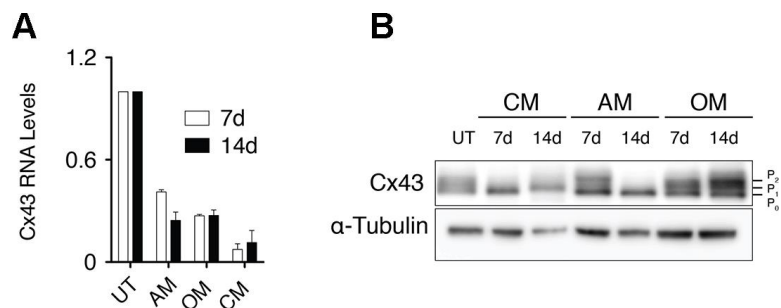https://doi.org/10.18632/aging.102866
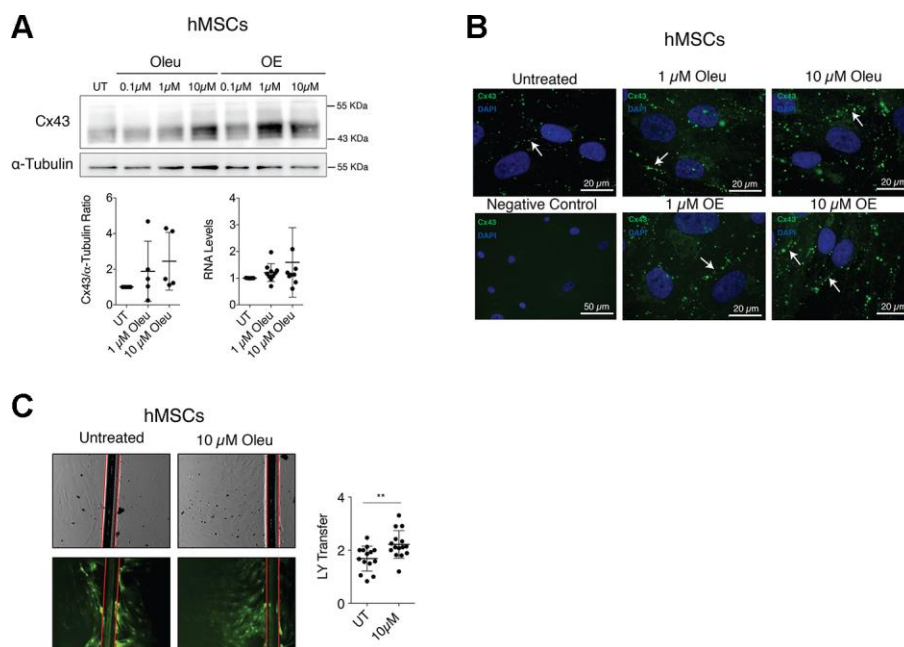PMID:32096765

Supplementary Figures

Supplementary Figure 1. Cell viability measured by MTT assay of (**A**) hMSCs from both bone marrow or subcutaneous inguinal fat (n=5 independent experiments, P=0.1065) and (**B**) chondrocytes (n=6 independent experiments, P=0.7871) exposed to different concentrations of oleuropein (Oleu) for 17 h. Data is expressed as mean±SD, one-way ANOVA. *P<0.05, **P<0.01 and ***P<0.0001.
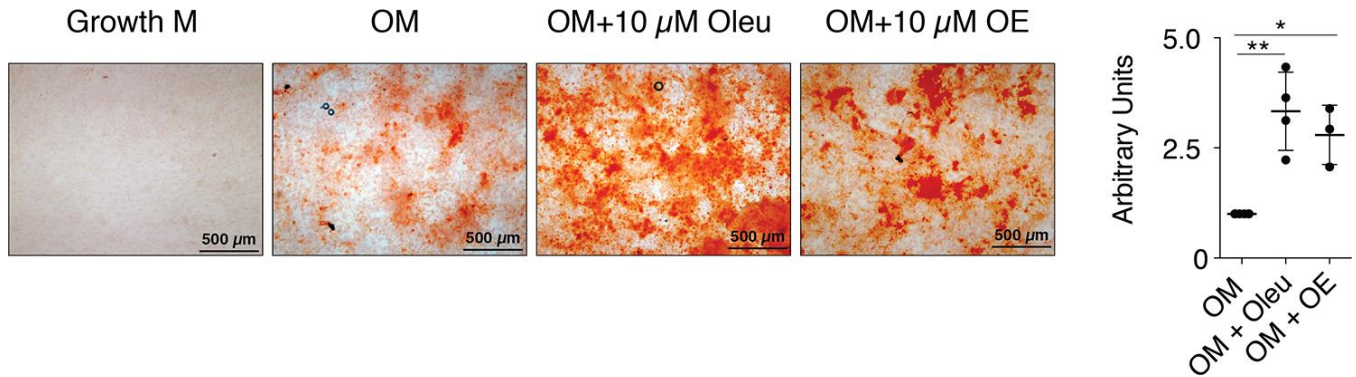

Supplementary Figure 2. (**A**) Adipogenic differentiation of hMSCs exposed to different concentrations of oleuropein (Oleu) or OE. Cells were stained with oil red O for lipid evaluation. The graph represents the ratio of cells with lipid deposits to the total number of cells and was normalized to hMSCs cultured in adipogenic medium (AM) (n=3-9 independent experiments, P<0.0001). (**B**) Osteogenic differentiation of hMSCs treated with oleuropein or OE for 21 days. Alizarin red staining was performed to evaluate calcium deposits. Quantification was normalized to hMSCs cultured in osteogenic medium (OM) (n=4-6 independent experiments, P=0.0166). (**C**) Chondrogenic differentiation of hMSCs for 30 days exposed to different concentrations of oleuropein or OE. Images represent Col2A1 immunohistochemistry (n=4-7 independent experiments, P=0.0609). (**D**) Images showing the phenotypes of hMSCs differentiated for 14 days with or without oleuropein. AM (adipogenic differentiation), OM (osteogenesis) and CM (chondrogenesis). Data is expressed as mean±SD, one-way ANOVA, *P<0.05, **P<0.01 and ***P<0.0001.
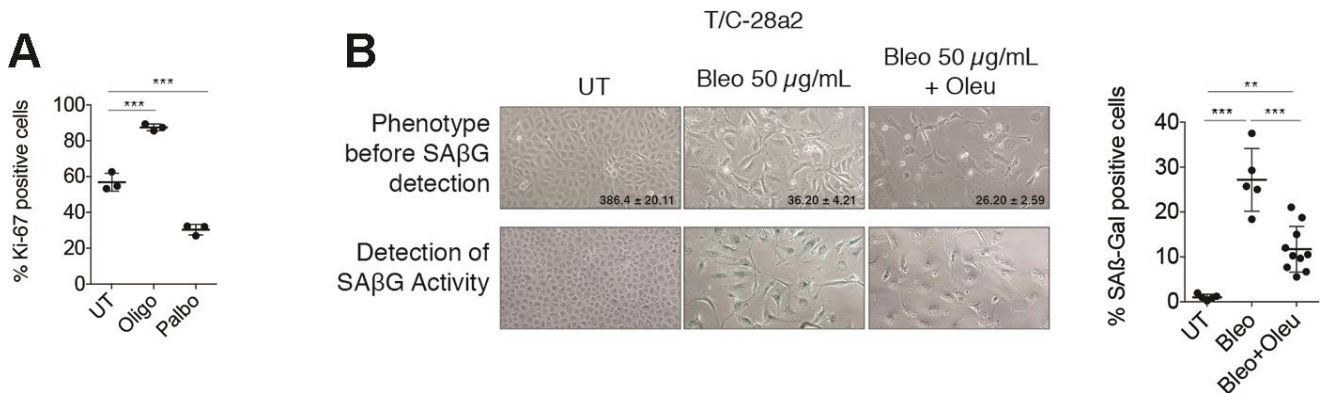
Supplementary Figure 3. (**A**) Cx43 levels analyzed by RT-qPCR of hMSCs differentiated with adipogenic (AM), osteogenic (OM) or chondrogenic (CM) medium for 7 and 14 days (n=2-3 independent experiments; data were normalized to HPRT-1 levels and are shown as mean±SD). (**B**) Comparative Cx43 protein levels of hMSCs cultured in chondrogenic (CM), adipogenic (AM) and osteogenic medium (OM) for 7 and 14 days. α-tubulin was used as a loading control.

Supplementary Figure 4. (**A**) Western blot showing increased Cx43 protein expression in hMSCs obtained from bone marrow and subcutaneous inguinal fat and treated for 2 h with oleuropein or olive-extract (OE) containing 41.5% Oleu as well as other polyphenolic compounds. α-tubulin was used as a loading control (n=5 independent experiments; one-way ANOVA, P=0.2723). RT-qPCR showing increased Cx43 mRNA in hMSCs treated with Oleu in basal/growth medium (α-MEM with 10% FBS) (n=9 independent experiments; data were normalized to HPRT-1 levels; one-way ANOVA, P=0.1041). (**B**) Immunofluorescence analysis showing increased Cx43 at the membrane (GJ plaques, white arrows) in hMSCs treated with oleuropein or OE for 2 h. Cell nuclei were stained with DAPI. Original magnifications ×40 and ×100. Images represent two independent experiments. (**C**) SL/DT assay examining GJ activity in hMSCs treated with 10 μM Oleu or 10 μM OE. Red lines represent the cut edge where cells took up the LY immediately after scraping. The graph represents the ratio of stained cells to the number of cells at the scrape edge (n=10 independent experiments; Student's t test, P=0.0087). Data is expressed as mean±SD, *P<0.05, **P<0.01 and ***P<0.0001.

Supplementary Figure 5. Calcium deposits in osteogenic medium-differentiated OACs evaluated by alizarin red staining. OACs were cultured in osteogenic medium (OM) supplemented with 10 µM oleuropein (Oleu) or OE for 21 days. Quantification was performed by counting red pixels and normalization to hMSCs differentiated in osteogenic medium without treatment. n=3 technical replicates; mean±SD; one-way ANOVA with *P*=0.0023.

Supplementary Figure 6. (**A**) Cell proliferation was evaluated in the T/C-28a2 chondrocyte cell line by Ki-67 immunofluorescence after oligomycin or Palbociclib treatment (n=3 independent experiments; mean±SD; one-way ANOVA with *P*<0.0001). (**B**) T/C-28a2 chondrocyte cell line was cultured with 50 µg/mL of bleomycin for 24 h, and then cultured in normal growth medium or in the presence of oleuropein 10 µg/mL for another 24 h. The mean mean±SD of the number of cells from 5 different visual fields are shown. ß-galactosidase activity was detected by X-Gal cleavage, and cell staining (blue) was evaluated by microscopy. Quantification is shown on the right (n=5-10 technical replicates; mean±SD; one-way ANOVA with *P*<0.0001).

Supplementary Tables

Supplementary Table 1. List of antibodies used in flow cytometry assays.

Antibody	Fluorochrome	Reference	Source	Laser (nm)	Filter	Dilution
CD105	PE	105PE-100T	Immunostep	488	585/42	1:50
CD166	APC	1399990314	Immunostep	635	661/16	1:100
Cx43	APC	FAB7737A	R&D	635	661/16	1:50

Supplementary Table 2. List of primer sequences (5'–3') used for RT-PCR analysis.

Gene name (protein name)	Forward	Reverse
ACAN (Aggrecan)	CAGAACAACTCGGGGAACAT	GCACAATTGGAACCCTGACT
Cdkn2a (p16^{Ink4a})	GAGCAGAACGATAGGGCTTG	CATGTGCCCTCTCCTCCTAA
GJA1 (Cx43)	ACATGGGTGACTGGAGCGCC	ATGATCTGCAGGACCCAGAA
HPRT-1 (HPRT-1)	TTGAGTTTGGAAACATCTGGAG	GCCCAAAGGGAACTGATAGTC
IL-1ß (IL-1ß)	CGAATCTCCGACCACCACTAC	TCCATGGCCACAACAACTGA
IL-6 (IL-6)	TGTAGCCGCCCCACACA	GGATGTACCGAATTTGTTTGTA
MMP-3 (MMP-3)	CCCTGGGTCTCTTTCACTCA	GCTGACAGCATCAAAGGACA
CDH2 (N-cadherin)	TATTTCCATCCTGCGTGTGA	GCGTTTCATCCATACCACAA
OSTCN (Osteocalcin)	CCATGAGAGCCCTCACACTCC	GGTCAGCCAACTCGTCACAGTC
PPARG (PPARγ)	GCGATTCCTTCACTGATACACTG	GAGTGGGAGTGGTCTTCCATTAC
PTGS2 (COX-2)	CTTCACGCATCAGTTTTTCAAG	TCACCGTAAATATGATTTAAGTCCAC
TWIST1 (Twist-1)	CATGTCCGCGTCCCACTA	CACGCCCTGTTTCTTTGAAT
VIM (Vimentin)	ACTTTGCCGTTGAAGCTG	AATCCAGATTAGTTTCCCTCAGGT